Lecture IV+V: Many-Body Methods for Nuclear Structure

Morten Hjorth-Jensen[1,2]

[1]Department of Physics and Center of Mathematics for Applications
University of Oslo, N-0316 Oslo

[2]Department of Physics and Astronomy, Michigan State University
East Lansing, Michigan, USA

January 23, 2009

Outline

Outline

Outline

Outline

Why Coupled-Cluster theory?

Advantages

- Fully microscopic. Only linked diagrams enter, size extensive
- Can be improved upon systematically, e.g., by inclusion of three-body interactions and more complicated correlations. To be contrasted to many-body perturbation theory.
- Allows for description of both closed-shell systems and valence systems
- Derivation of effective two and three-body interactions for the shell model
- Amenable to parallel computing
- Huge development in Quantum Chemistry. Exploit this for the nuclear many-body problem.

Why Coupled-Cluster theory?

Advantages

- Fully microscopic. Only linked diagrams enter, size extensive
- Can be improved upon systematically, e.g., by inclusion of three-body interactions and more complicated correlations. To be contrasted to many-body perturbation theory.
- Allows for description of both closed-shell systems and valence systems
- Derivation of effective two and three-body interactions for the shell model
- Amenable to parallel computing
- Huge development in Quantum Chemistry. Exploit this for the nuclear many-body problem.

Why Coupled-Cluster theory?

Advantages

- Fully microscopic. Only linked diagrams enter, size extensive
- Can be improved upon systematically, e.g., by inclusion of three-body interactions and more complicated correlations. To be contrasted to many-body perturbation theory.
- Allows for description of both closed-shell systems and valence systems
- Derivation of effective two and three-body interactions for the shell model
- Amenable to parallel computing
- Huge development in Quantum Chemistry. Exploit this for the nuclear many-body problem.

Why Coupled-Cluster theory?

Advantages

- Fully microscopic. Only linked diagrams enter, size extensive
- Can be improved upon systematically, e.g., by inclusion of three-body interactions and more complicated correlations. To be contrasted to many-body perturbation theory.
- Allows for description of both closed-shell systems and valence systems
- Derivation of effective two and three-body interactions for the shell model
- Amenable to parallel computing
- Huge development in Quantum Chemistry. Exploit this for the nuclear many-body problem.

Why Coupled-Cluster theory?

Advantages

- Fully microscopic. Only linked diagrams enter, size extensive
- Can be improved upon systematically, e.g., by inclusion of three-body interactions and more complicated correlations. To be contrasted to many-body perturbation theory.
- Allows for description of both closed-shell systems and valence systems
- Derivation of effective two and three-body interactions for the shell model
- Amenable to parallel computing
- Huge development in Quantum Chemistry. Exploit this for the nuclear many-body problem.

Why Coupled-Cluster theory?

Advantages

- Fully microscopic. Only linked diagrams enter, size extensive
- Can be improved upon systematically, e.g., by inclusion of three-body interactions and more complicated correlations. To be contrasted to many-body perturbation theory.
- Allows for description of both closed-shell systems and valence systems
- Derivation of effective two and three-body interactions for the shell model
- Amenable to parallel computing
- Huge development in Quantum Chemistry. Exploit this for the nuclear many-body problem.

More on Coupled Cluster

More advantages

- Can be used to generate excited spectra for nuclei like ^{16}O or ^{40}Ca with many shells. Hard for the shell model to go beyond one major shell. Huge dimensionalities in shell-model calcs

System	4 shells	7 shells
^{4}He	4E4	9E6
^{8}B	4E8	5E13
^{12}C	6E11	4E19
^{16}O	3E14	9E24

Shell-model codes can today reach dimensionalities of $d \sim 10^{10}$ basis states.

- Can include complex effective interactions

More on Coupled Cluster

More advantages

- Can be used to generate excited spectra for nuclei like ^{16}O or ^{40}Ca with many shells. Hard for the shell model to go beyond one major shell. Huge dimensionalities in shell-model calcs

System	4 shells	7 shells
^{4}He	4E4	9E6
^{8}B	4E8	5E13
^{12}C	6E11	4E19
^{16}O	3E14	9E24

Shell-model codes can today reach dimensionalities of $d \sim 10^{10}$ basis states.

- Can include complex effective interactions

Ab-initio approaches to light and medium mass nuclei

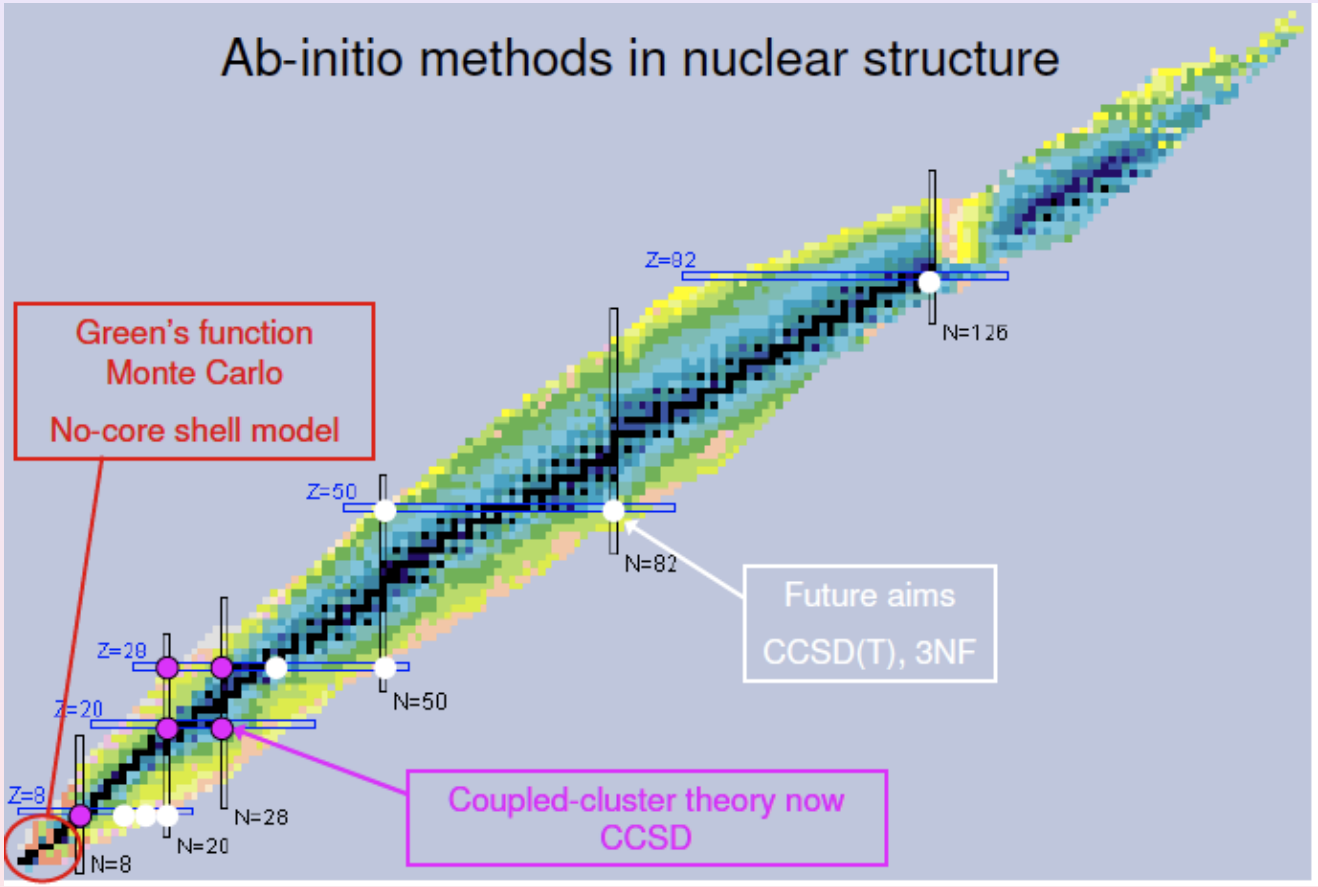

Coupled Cluster Theory

Exponential Ansatz for Ψ

$$|\Psi\rangle = e^{\hat{T}}|\Phi_0\rangle, \quad \hat{T} = \hat{T}_1 + \hat{T}_2 + \ldots + \hat{T}_A$$

$$\hat{T}_1 = \sum_{i,a} t_i^a \hat{a}_a^\dagger \hat{a}_i, \; \hat{T}_2 = \frac{1}{2} \sum_{i<j,a<b} t_{ij}^{ab} \hat{a}_a^\dagger \hat{a}_b^\dagger \hat{a}_j \hat{a}_i.$$

Coupled Cluster Equations

$$\Delta E = \langle \Phi_0 | \left(H_N exp(T) \right)_C | \Phi_0 \rangle$$

$$0 = \langle \Phi_p | \left(H_N exp(T) \right)_C | \Phi_0 \rangle$$

$$\bar{H} = \left(H_N exp(T) \right)_C$$

1. Coupled Cluster Theory is fully microscopic .
2. Coupled Cluster is size extensive. No unlinked diagrams enters, and error scales linearly with number of particles.
3. Low computational cost (CCSD scales as $n_o^2 n_u^4$).
4. Capable of systematic improvements.
5. Amenable to parallel computing.

Coupled Cluster, Basics

The single-reference coupled-cluster theory is based on the exponential ansatz for the ground-state wave function of the A-body system,

$$|\Psi_0^{(A)}\rangle = e^{T^{(A)}}|\Phi\rangle, \tag{1}$$

where $T^{(A)}$ is the cluster operator (a p-h excitation operator) and $|\Phi\rangle$ is the corresponding reference determinant (defining the Fermi vacuum) obtained by performing some mean-field calculation or by simply filling A lowest-energy single-particle states Superscripts, such as (A), indicate the number of particles in a system under consideration, at the relevant operators and energies.

Formally, this equation is a direct consequence of the connected-cluster theorem, first clearly stated by Hubbard, which is, in turn, related to the linked cluster theorem of many-body perturbation theory. According to the connected-cluster theorem, the cluster operator $T^{(A)}$ generates connected wave function diagrams summed through infinite order. Operationally, $T^{(A)}$ is a simple many-body excitation operator, which in all standard coupled-cluster approximations is truncated at a given (usually low) p-h excitation level $M < A$.

Coupled Cluster, Basics

The general form of the truncated cluster operator, defining a standard single-reference coupled-cluster approximation characterized by the excitation level M, is

$$T^{(A)}(M) = \sum_{n=1}^{M} T_n, \tag{2}$$

where

$$T_n = \left(\frac{1}{n!}\right)^2 t^{i_1 \dots i_n}_{a_1 \dots a_n} \, a^{a_1} \cdots a^{a_n} a_{i_n} \cdots a_{i_1} \tag{3}$$

are the many-body components of $T^{(A)}(M)$, and $t^{i_1 \dots i_n}_{a_1 \dots a_n}$ are the corresponding cluster amplitudes.

Coupled Cluster, Basics

The cluster amplitudes $t_{a_1\dots a_n}^{i_1\cdots i_n}$ are determined by solving a coupled system of nonlinear and energy-independent algebraic equations of the form:

$$\langle \Phi_{i_1\dots i_n}^{a_1\cdots a_n} | \bar{H}_N(M) | \Phi \rangle = 0, \quad i_1 < \cdots < i_n, \;\; a_1 < \cdots < a_n, \tag{4}$$

where $n = 1, \dots, M$. Here,

$$\bar{H}_N(M) = e^{-T^{(A)}(M)} H_N \, e^{T^{(A)}(M)} = (H_N \, e^{T^{(A)}(M)})_C \tag{5}$$

is the similarity-transformed Hamiltonian of the coupled-cluster theory truncated at *Mp-Mh* excitations, subscript C designates the connected part of the corresponding operator expression, and $|\Phi_{i_1\dots i_n}^{a_1\cdots a_n}\rangle \equiv a^{a_1} \cdots a^{a_n} a_{i_n} \cdots a_{i_1} |\Phi\rangle$ are the *np-nh* or *n*-tuply excited determinants relative to $|\Phi\rangle$.

Coupled Cluster, Basics

The basic CCSD (coupled-cluster singles and doubles) method corresponds to $M = 2$ and the cluster operator $T^{(A)}$ is approximated by

$$T^{(A)}(\mathrm{CCSD}) \equiv T^{(A)}(2) = T_1 + T_2, \tag{6}$$

where

$$T_1 = t_a^i a^a a_i \tag{7}$$

and

$$T_2 = \tfrac{1}{4}\, t_{ab}^{ij} a^a a^b a_j a_i \tag{8}$$

are $1p$-$1h$ or singly excited and $2p$-$2h$ or doubly excited cluster components, t_a^i and t_{ab}^{ij} are the corresponding singly and doubly excited cluster amplitudes, and $i, j, \ldots$ $(a, b, \ldots)$ are the single-particle states occupied (unoccupied) in the reference determinant $|\Phi\rangle$.

Coupled Cluster, Basics

The standard CCSD equations for the singly and doubly excited cluster amplitudes t_a^i and t_{ab}^{ij}, defining T_1 and T_2, respectively, can be written as

$$\langle \Phi_i^a | \bar{H}_N(\mathrm{CCSD}) | \Phi \rangle = 0, \tag{9}$$

$$\langle \Phi_{ij}^{ab} | \bar{H}_N(\mathrm{CCSD}) | \Phi \rangle = 0, \quad i < j,\ a < b, \tag{10}$$

where

$$\begin{aligned} \bar{H}_N(\mathrm{CCSD}) &\equiv \bar{H}_N(2) = e^{-T^{(A)}(\mathrm{CCSD})} H_N\, e^{T^{(A)}(\mathrm{CCSD})} \\ &= (H_N\, e^{T^{(A)}(\mathrm{CCSD})})_C \end{aligned} \tag{11}$$

is the similarity-transformed Hamiltonian of the CCSD approach.

Coupled Cluster, Basics

The system of coupled-cluster equations, is obtained in the following way.
We first insert the coupled-cluster wave function $|\Psi_0^{(A)}\rangle$ into the A-body Schrödinger equation,

$$H_N|\Psi_0^{(A)}\rangle = \Delta E_0^{(A)}|\Psi_0^{(A)}\rangle, \tag{12}$$

where

$$\Delta E_0^{(A)} = E_0^{(A)} - \langle\Phi|H|\Phi\rangle$$

is the corresponding energy relative to the reference energy $\langle\Phi|H|\Phi\rangle$, and premultiply both sides on the left by $e^{-T^{(A)}}$ to obtain the connected-cluster form of the Schrödinger equation

$$\bar{H}_N|\Phi\rangle = \Delta E_0^{(A)}|\Phi\rangle, \tag{13}$$

where

$$\bar{H}_N = e^{-T^{(A)}} H_N e^{T^{(A)}} = (H_N e^{T^{(A)}})_C \tag{14}$$

is the similarity-transformed Hamiltonian.

Coupled Cluster, Basics

Next, we project Eq. (13), in which $T^{(A)}$ is replaced by its approximate form $T^{(A)}(M)$, Eq. (2), onto the excited determinants $|\Phi^{a_1\cdots a_n}_{i_1\ldots i_n}\rangle$, corresponding to the p-h excitations included in $T^{(A)}(M)$. The excited determinants $|\Phi^{a_1\cdots a_n}_{i_1\ldots i_n}\rangle$ are orthogonal to the reference determinant $|\Phi\rangle$, so that we end up with nonlinear and energy-independent algebraic equations of the form of Eq. (4).

Coupled Cluster, Basics

Once the system of equations, Eq. (4), is solved for $T^{(A)}(M)$ or $t^{i_1\ldots i_n}_{a_1\ldots a_n}$ (or Eqs. (9) and (10) are solved for T_1 and T_2 or t^i_a and t^{ij}_{ab}), the ground-state coupled-cluster energy is calculated using the equation

$$\begin{aligned} E_0^{(A)}(M) &= \langle\Phi|H|\Phi\rangle + \Delta E_0^{(A)}(M) \\ &= \langle\Phi|H|\Phi\rangle + \langle\Phi|\bar{H}_N(M)|\Phi\rangle \\ &= \langle\Phi|H|\Phi\rangle + \langle\Phi|\bar{H}_{N,\mathrm{close}}(M)|\Phi\rangle, \end{aligned} \tag{15}$$

where $\bar{H}_{N,\mathrm{close}}(M)$ is the closed part of $\bar{H}_N(M)$ which is represented by those diagrams contributing to $\bar{H}_N^{(M)}$ that have no external (uncontracted) Fermion lines.

Coupled Cluster, Basics

It can easily be shown that if H contains only up to two-body interactions and $2 \leq M \leq A$, we can write

$$E_0^{(A)}(M) = \langle \Phi | H | \Phi \rangle + \langle \Phi | [H_N(T_1 + T_2 + \tfrac{1}{2} T_1^2)]_C | \Phi \rangle. \tag{16}$$

In other words, we only need T_1 and T_2 clusters to calculate the ground-state energy $E_0^{(A)}(M)$ of the A-body ($A \geq 2$) system even if we solve for other cluster components T_n with $n > 2$. As long as the Hamiltonian contains up to two-body interactions, the above energy expression is correct even in the exact case, when the cluster operator T is not truncated.

Coupled Cluster, Equations

To see this we compute the expectation of the energy from

$$E = \langle \Psi_0 \mid \exp(-T) H \exp(T) \mid \Psi_0 \rangle .$$

In addition, if we stop at the Singles and Doubles level we have the equations for the amplitudes are found by left projection of excited Slater determinants so that

$$0 = \langle \Psi_i^a \mid \exp(-T) H(T) \mid \Psi_0 \rangle ,$$

$$0 = \langle \Psi_{ij}^{ab} \mid \exp(-T) H(T) \mid \Psi_0 \rangle .$$

The Baker-Campbell-Hausdorf relation

$$\begin{aligned} \exp(-T) H(T) &= H + [H, T_1] + [H, T_2] \\ &+ \frac{1}{2} [[H, T_1], T_1] + \frac{1}{2} [[H, T_2], T_2] \\ &+ [[H, T_1], T_2] + \cdots . \end{aligned}$$

can be used to terminate exactly at quadruply nested commutators when the Hamiltonian contains at most two-body terms.

Coupled Cluster, Basics

The nonlinear character of the system of coupled-cluster equations of the form of Eq. (4) does not mean that the resulting equations contain very high powers of $T^{(A)}(M)$. For example, if the Hamiltonian H does not contain higher–than–pairwise interactions, the CCSD equations for the T_1 and T_2 clusters, or for the amplitudes t_a^i and t_{ab}^{ij} that represent these clusters, become

$$\langle \Phi_i^a | [H_N(1 + T_1 + T_2 + \tfrac{1}{2}T_1^2 + T_1T_2 + \tfrac{1}{6}T_1^3)]_C | \Phi \rangle = 0, \tag{17}$$

$$\begin{aligned} \langle \Phi_{ij}^{ab} | \quad & [H_N(1 + T_1 + T_2 + \tfrac{1}{2}T_1^2 + T_1T_2 + \tfrac{1}{6}T_1^3 \\ & + \tfrac{1}{2}T_2^2 + \tfrac{1}{2}T_1^2T_2 + \tfrac{1}{24}T_1^4)]_C | \Phi \rangle = 0. \end{aligned} \tag{18}$$

Coupled Cluster, Basics

The explicitly connected form of the coupled-cluster equations, such as Eqs. (4) or (17) and (18), guarantees that the process of solving these equations leads to connected terms in cluster components T_n and connected terms in the energy $E_0^{(A)}(M)$, independent of the truncation scheme M used to define $T^{(A)}(M)$. The absence of disconnected terms in $T^{(A)}(M)$ and $E_0^{(A)}(M)$ is essential to obtain the rigorously size-extensive results.

Coupled Cluster with Triple Correlations

Correlated many-body wave function is given by

$$| \Psi \rangle = \exp(T) | \Phi_0 \rangle ,$$

with the reference Slater determinant as $| \Phi_0 \rangle$ and the correlation operator as $T = T_1 + T_2 + T_3 + \cdots + T_A$

$$T_1 = \sum_{i<\varepsilon_f, a>\varepsilon_f} t_i^a a_a^+ a_i$$

for single excitations (S, 1p-1h)

$$T_2 = \frac{1}{4} \sum_{i,j<\varepsilon_f; ab>\varepsilon_f} t_{ij}^{ab} a_a^+ a_b^+ a_j a_i$$

for double excitations (D, 2p-2h) and

$$T_3 = \frac{1}{36} \sum_{i,jk<\varepsilon_f; abc>\varepsilon_f} t_{ijk}^{abc} a_a^+ a_b^+ a_c^+ a_k a_j a_i$$

for triple excitations (T, 3p-3h)

Coupled Cluster equations

Define:

$$f = \sum_{pq} f_{pq} \{a_p^+ a_q\}$$

with f_{pq} the Fock matrix elements

$$W = \frac{1}{4} \sum_{pqrs} \langle pq||rs\rangle \{a_p^+ a_q^+ a_r a_s\}$$

where $\langle pq||rs\rangle$ are anti-symmetrized two-body matrix elements. Normal-order creation and annihilation operators.

Coupled Cluster, CCSDT level

The extention to triples gives the following equations for the amplitudes with 1p-1h

$$\langle \Phi_i^a | [fT_1 + f(T_2 + 1/2\,T_1^2) + WT_1 + W(T_2 + 1/2\,T_1^2) + W(T_1\,T_2 + 1/6\,T_1^3 + T_3)]_C |\Phi\rangle = 0,$$

and with 2p-2h

$$\langle \Phi_{ij}^{ab} | [fT_1 + f(T_3 + T_2\,T_1) + W + WT_1 + W(T_2 + 1/2\,T_1^2) + W(T_1\,T_2 + 1/6\,T_1^3 + T_3)$$

$$+ W(T_1\,T_3 + 1/2\,T_2^2 + 1/2\,T_2\,T_1^2 + 1/24\,T_1^4)]_C |\Phi\rangle = 0.$$

and with 3p-3h

$$\langle \Phi_{ijk}^{abc} | [fT_3 + f(T_3\,T_1 + 1/2\,T_2^2) + WT_2 + W(T_3 + T_1\,T_2) + W(1/2\,T_2 + T_3\,T_1 1/2\,T_1^2 + T_1)$$

$$+ W(T_2\,T_3 + 1/2\,T_2^2\,T_1 + 1/2\,T_3\,T_1^2 + 1/6\,T_2\,T_1^3)]_C |\Phi\rangle = 0.$$

Coupled Cluster

When the equations have been solved we have defined the amplitudes $t^{\cdots}_{\cdots}$

$$T_1 = \sum_{i<\varepsilon_f, a>\varepsilon_f} t_i^a a_a^+ a_i$$

$$T_2 = \frac{1}{4} \sum_{i,j<\varepsilon_f; ab>\varepsilon_f} t_{ij}^{ab} a_a^+ a_b^+ a_j a_i$$

$$T_3 = \frac{1}{36} \sum_{i,jk<\varepsilon_f; abc>\varepsilon_f} t_{ijk}^{abc} a_a^+ a_b^+ a_c^+ a_k a_j a_i$$

and can then extract effective interactions. Different approximations to the solution of the triples equations yield different CCSDT approximations. CCSD scales as $n_o^2 n_u^4$ while full CCSDT scales as $n_o^3 n_u^5$, with n_o the number of occupied orbits and n_u the number of unoccupied.

CCSD acronyms

1. CCSD(T) : CCSD energy is augmented by a perturbative treatment of triple excitation effects, normally reliable.
2. CCSDT-1: skip WT_1T_3 in 2p-2h part and keep only fT_3 and WT_2 in 3p-3h
3. CCSDT-2: full 2p-2h and 3p-3h as in CCSDT-1
4. CCSDT-3 : All terms in 3p-3h except the fT_3 term.

Coupled Cluster in Pictures

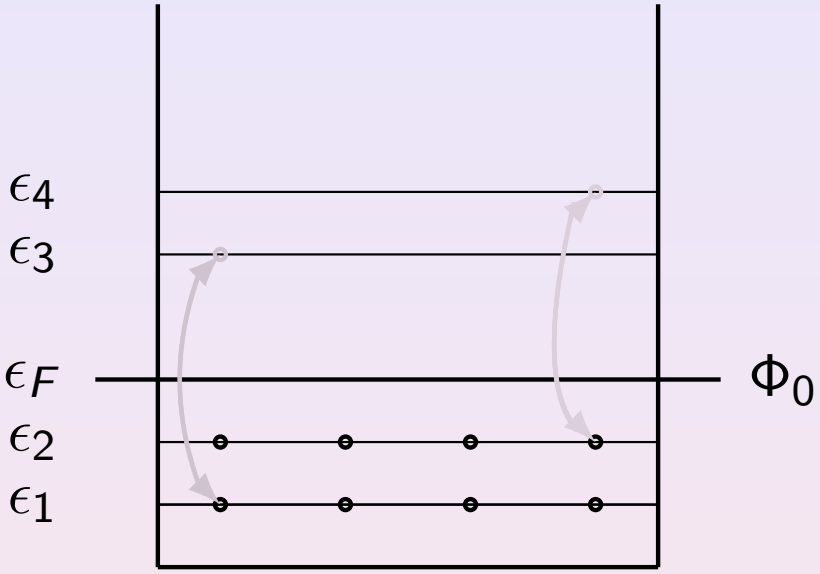

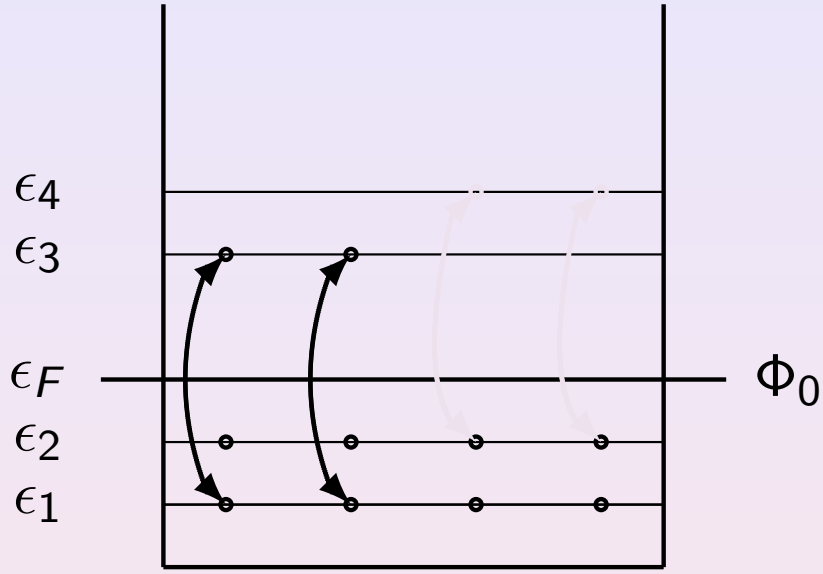

From T_1 to T_1^2

$$T_1 = \sum_{i<\epsilon_f, a>\epsilon_f} t_i^a a_a^+ a_i$$

From T_2 to T_2^2

$$T_2 = \sum_{i,j<\epsilon_f; ab>\epsilon_f} t_{ij}^{ab} a_a^+ a_b^+ a_j a_i$$

Coupled Cluster in Pictures

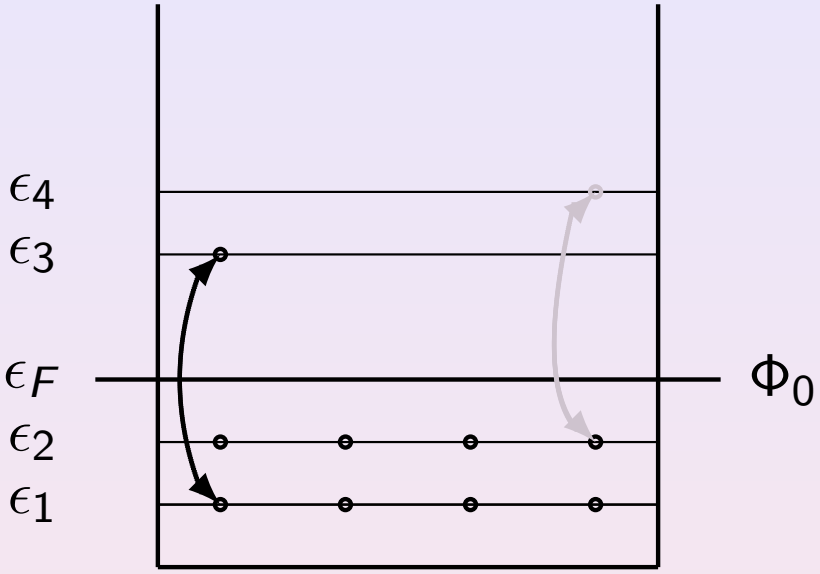

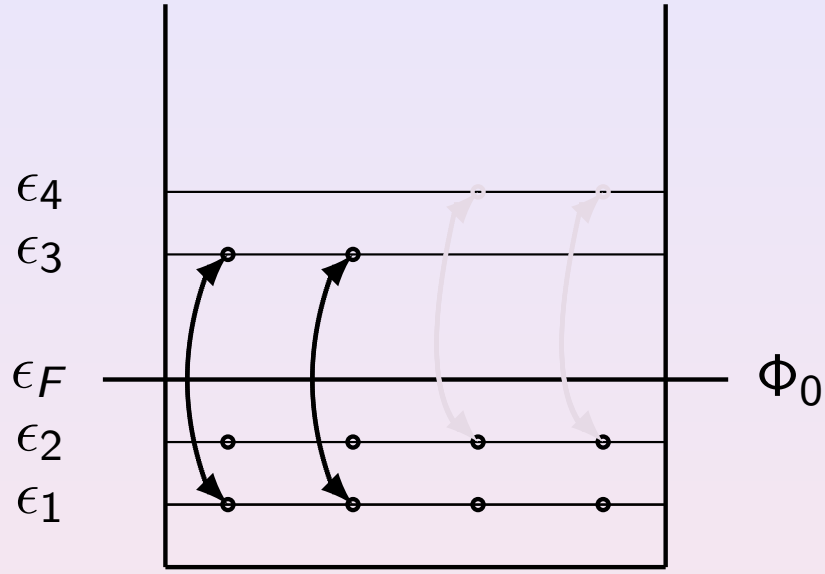

From T_1 to T_1^2

$$T_1 = \sum_{i<\varepsilon_f, a>\varepsilon_f} t_i^a a_a^+ a_i$$

From T_2 to T_2^2

$$T_2 = \sum_{i,j<\varepsilon_f; ab>\varepsilon_f} t_{ij}^{ab} a_a^+ a_b^+ a_j a_i$$

Coupled Cluster in Pictures

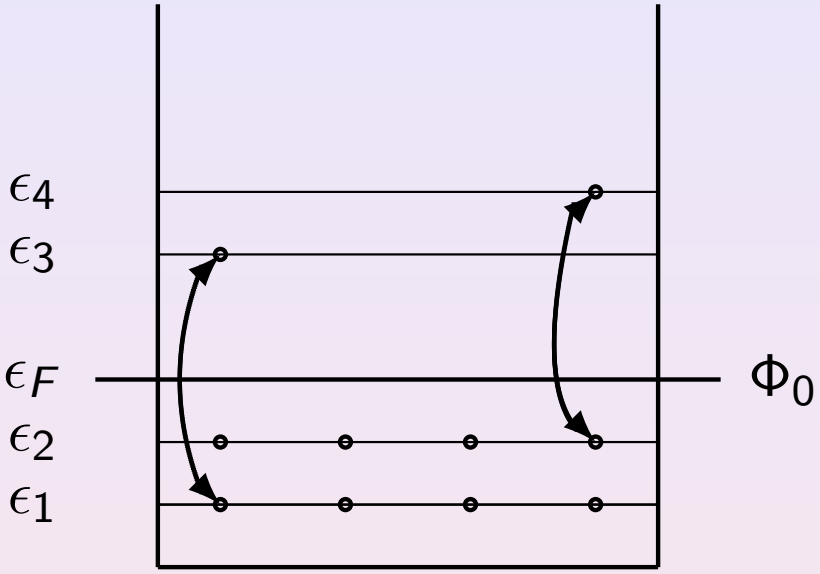

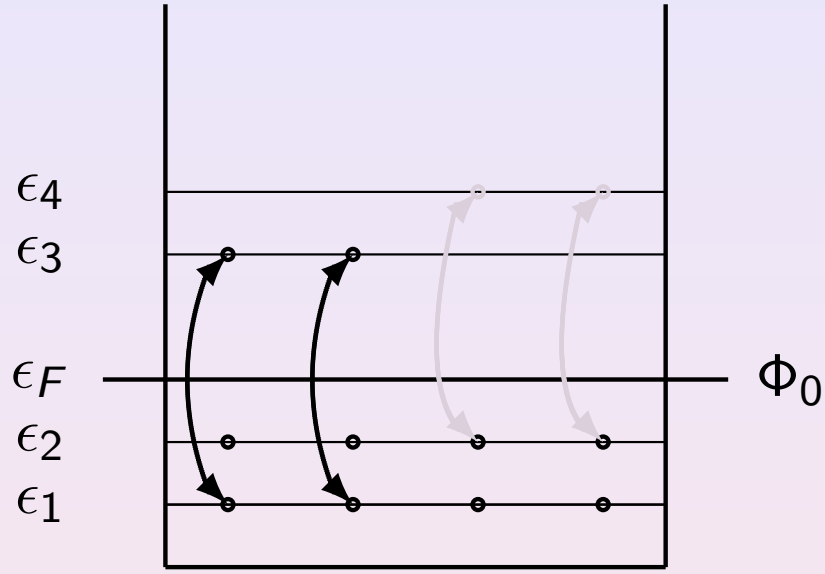

From T_1 to T_1^2

$T_1 = \sum_{i<\varepsilon_f, a>\varepsilon_f} t_i^a a_a^+ a_i$

From T_2 to T_2^2

$T_2 = \sum_{i,j<\varepsilon_f; ab>\varepsilon_f} t_{ij}^{ab} a_a^+ a_b^+ a_j a_i$

Coupled Cluster in Pictures

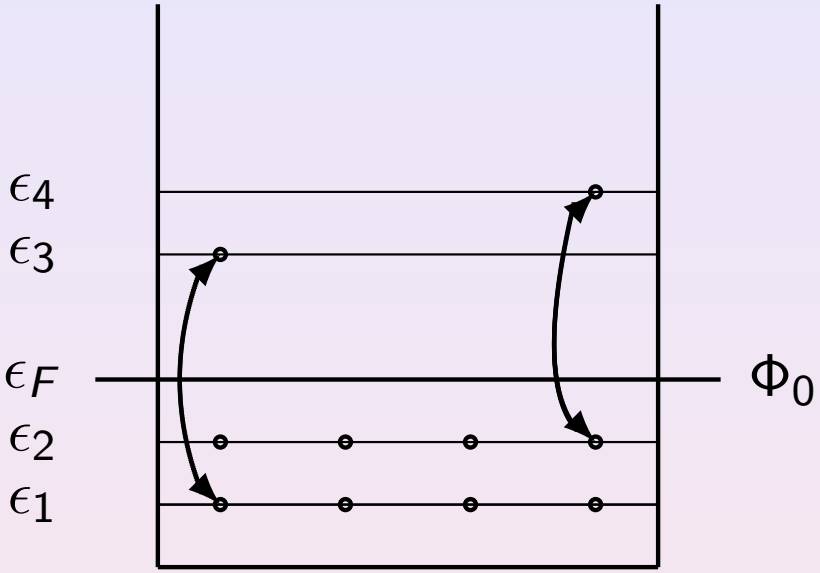

From T_1 to T_1^2

$$T_1 = \sum_{i<\varepsilon_f, a>\varepsilon_f} t_i^a a_a^+ a_i$$

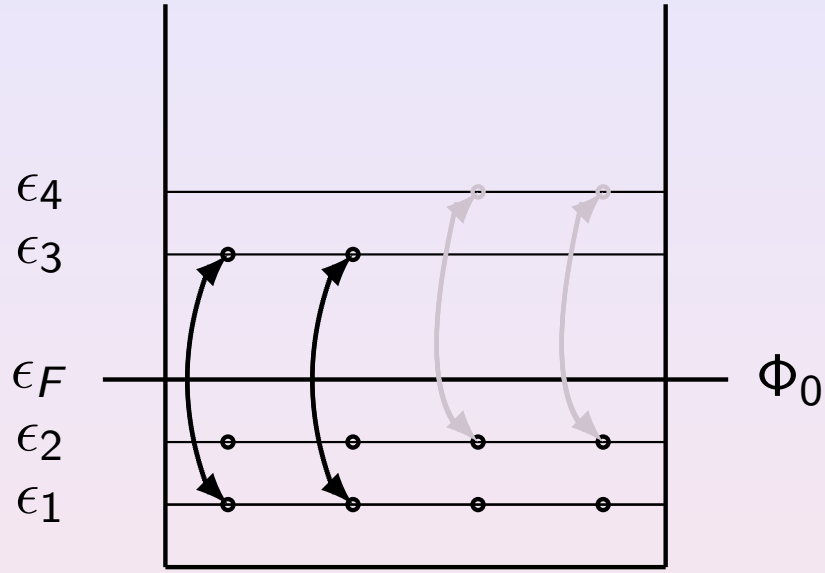

From T_2 to T_2^2

$$T_2 = \sum_{i,j<\varepsilon_f; ab>\varepsilon_f} t_{ij}^{ab} a_a^+ a_b^+ a_j a_i$$

Coupled Cluster in Pictures

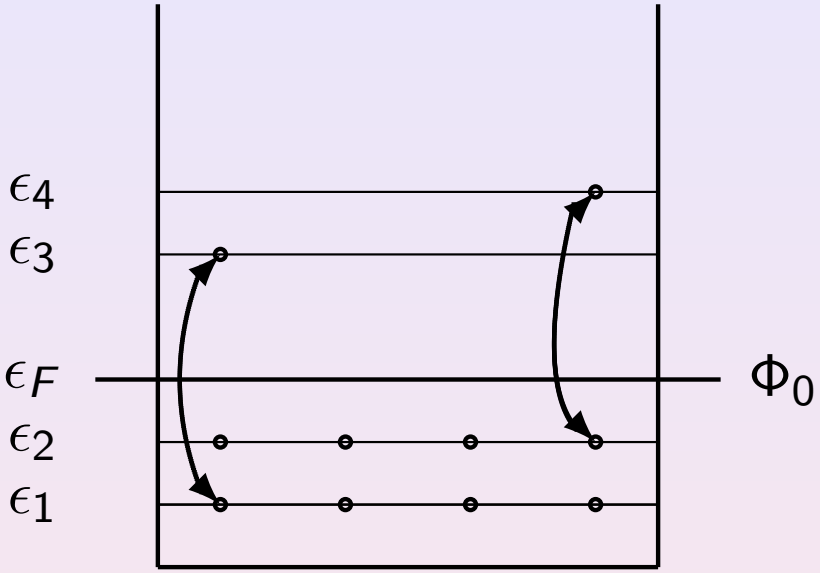

From T_1 to T_1^2

$$T_1 = \sum_{i<\varepsilon_f, a>\varepsilon_f} t_i^a a_a^+ a_i$$

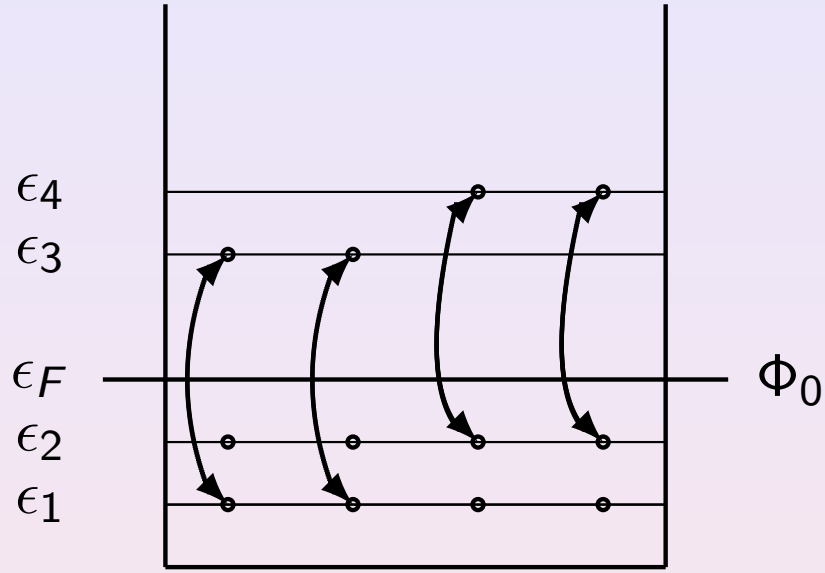

From T_2 to T_2^2

$$T_2 = \sum_{i,j<\varepsilon_f; ab>\varepsilon_f} t_{ij}^{ab} a_a^+ a_b^+ a_j a_i$$

More Coupled Cluster in Pictures

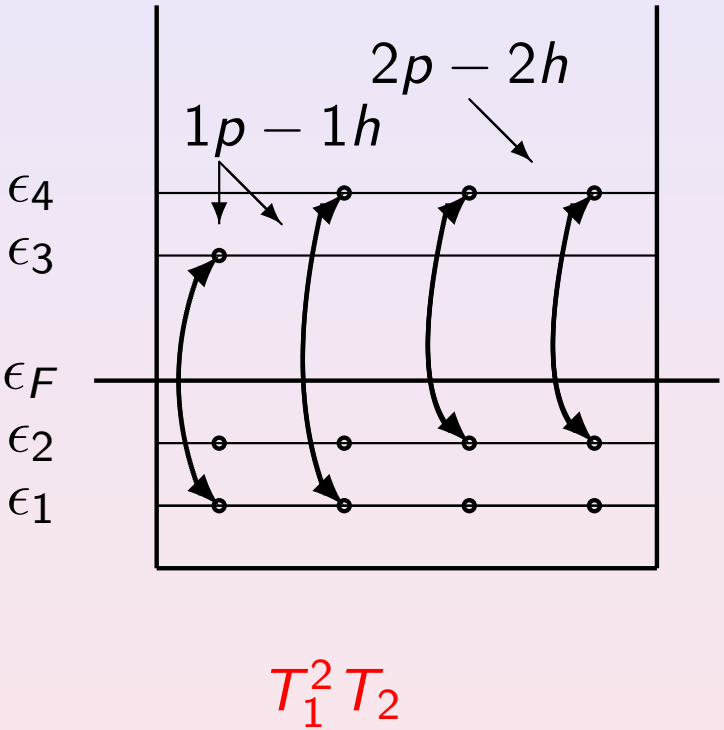

$T_1^2 T_2$

CCSD and Shell-Model Truncations

- Truncated shell model with $2p-2h$ has $\Psi_{2p-2h} = (1 + T_1 + T_2)\Phi_0$
- Energy contains then

$$E_{2p-2h} =$$

$$\langle \Phi_0(1+T_1^\dagger+T_2^\dagger)|H|(1+T_1+T_2)\Phi_0\rangle$$

- But CCSD has also $T_1^2 T_2$. Not in truncated shell model. Crucial.

Triples and ^{16}O

4 Major Shells, $0s0p1s0d1p0f$

The ground-state energy of ^{16}O calculated using various coupled cluster methods and oscillator basis states. CISD is shell-model with $2p-2h$, CISDT is shell-model with $3p-3h$ and CISDTQ is shell-model with $4p-4h$ truncations. Cannot go longer for shell model. Total shell-model dimension $d \sim 10^{14}$. Idaho-A interaction.

Method	Energy
CCSD	-139.310
CR-CCSD(T)	-139.621
CISD	-131.887
CISDT	-135.489
CISDTQ	-138.387

Size Matters! Role of size-extensivity

Goldstone's linked cluster theorem (1955)

Formal diagrammatic proof of Brueckner's conjecture that perturbation theory is size extensive. Only linked diagrams contribute to the energy of a (closed shell) nucleus. **Unlinked diagrams do not scale with mass number A and the sum of all unlinked diagrams is zero.**

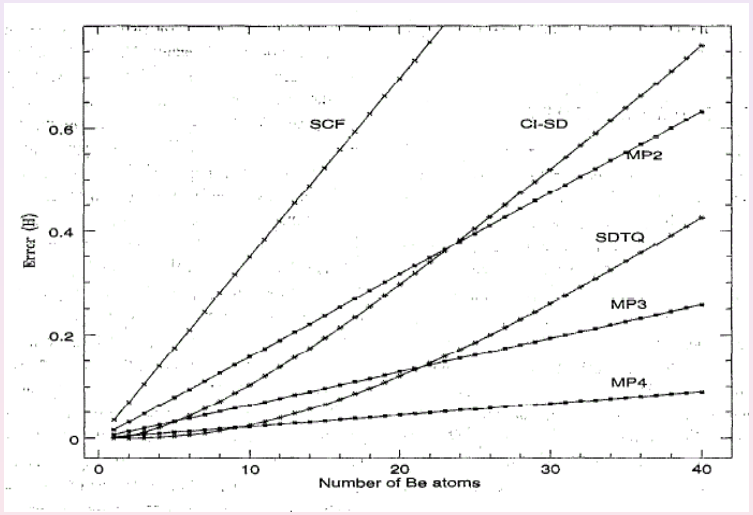

- **Size extensive theories:** Many-body perturbation theory, Full Configuration Interaction (FCI) and Coupled-cluster theory
- **Non-size extensive theories:** Particle-hole truncated shell-model (CISD, CISDT...)

Comparison with Shell Model/Configuration Interaction

In Shell Model approach a linear excitation operator is used instead of an exponential. $\Psi = (1 + B_1 + B_2 + ...)\Phi_0$

- Any particle-hole truncation introduces unlinked diagrams, and it is therefore not size extensive.
- Dimension increases dramatically with number of active particles.

Comparison of CC with CI at given excitation level.

Nuclear Example (Kowalski et al PRL 2004).

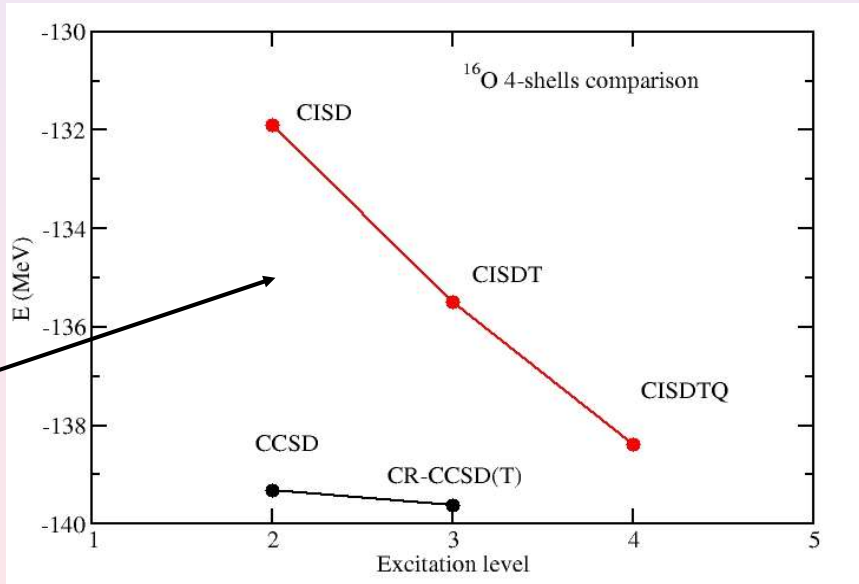

Relationship between shell model and CC amplitudes

$$B_1 = T_1$$

$$B_2 = T_2 + \frac{1}{2} T_1^2$$

$$B_3 = T_3 + T_2 T_1 + \frac{1}{6} T_1^3$$

$$B_4 = T_4 + T_3 T_1 + \frac{1}{2} T_2^2 + \frac{1}{2} T_2 T_1^2 + \frac{1}{24} T_1^4$$

$$\ldots$$

CCSD

CCSDT

Connected quadruples

Disconnected quadruples

Disagreement between CCM and IT-NCSM for ^{40}Ca

	Coupled-Cluster	IT-NCSM
^{16}O	-142.8 (CCSD) -148.2 (CCSD(T))	 -137.8 (4p-4h)
^{40}Ca	-491.2 (CCSD) -502.9 (CCSD(T))	-461.8 (3p-3h) -471.0 (4p-4h)

- Coupled-Cluster theory **size extensive**, energy scales correctly with size
- IT-NCSM is **not size extensive**. Can not judge the quality of a calculation of large system from the quality of a small (light) system.

Refs.:

1. Roth and Navratil PRL 99, 092501 (2007)
2. Hagen, Dean, Hjorth-Jensen, Papenbrock, Schwenk PRC 76, 044305 (2007)
3. Dean, Hagen, Hjorth-Jensen, Papenbrock, Schwenk PRL. 101, 119201 (2008) (comment)
4. Roth and Navratil, arxiv:0801.1484 (reply)

Spherical Coupled-Cluster Approach

1. Possible for nuclei with closed sub-shell (or cs ± 1)
2. Relatively simple since similarity transformed Hamiltonian is two-body (CCSD) or three-body (CCSDT) at most
3. Enourmous computational reduction: $n_o + n_u \rightarrow (n_o + n_u)^{2/3}$ (naive estimate)
   CCSD(T) for ^{40}Ca and ^{48}Ca on a single CPU (now)
   CCSDT for ^{48}Ca on many CPUs (future)
   CCSD(T) for ^{100}Sn and ^{132}Sn with "bare" chiral interactions on many CPUs.

$$\hat{T}_1 = \sum_{j_i, j_a} t_{j_i}^{j_a} (a_{j_a}^\dagger \times \tilde{a}_{j_i})^{(0)} ,$$

$$\hat{T}_2 = \sum_{j_i, j_j, j_a, j_b, J} t_{j_i, j_j}^{j_a, j_b}(J) (a_{j_a}^\dagger \times a_{j_b}^\dagger)^{(J)} \cdot (\tilde{a}_{j_j} \times \tilde{a}_{j_i})^{(J)} .$$

j_i and j_a denote the spin of the occupied and unoccupied subshells.

^{16}O, ^{40}Ca, ^{48}Ca and ^{48}Ni with "bare" chiral interactions

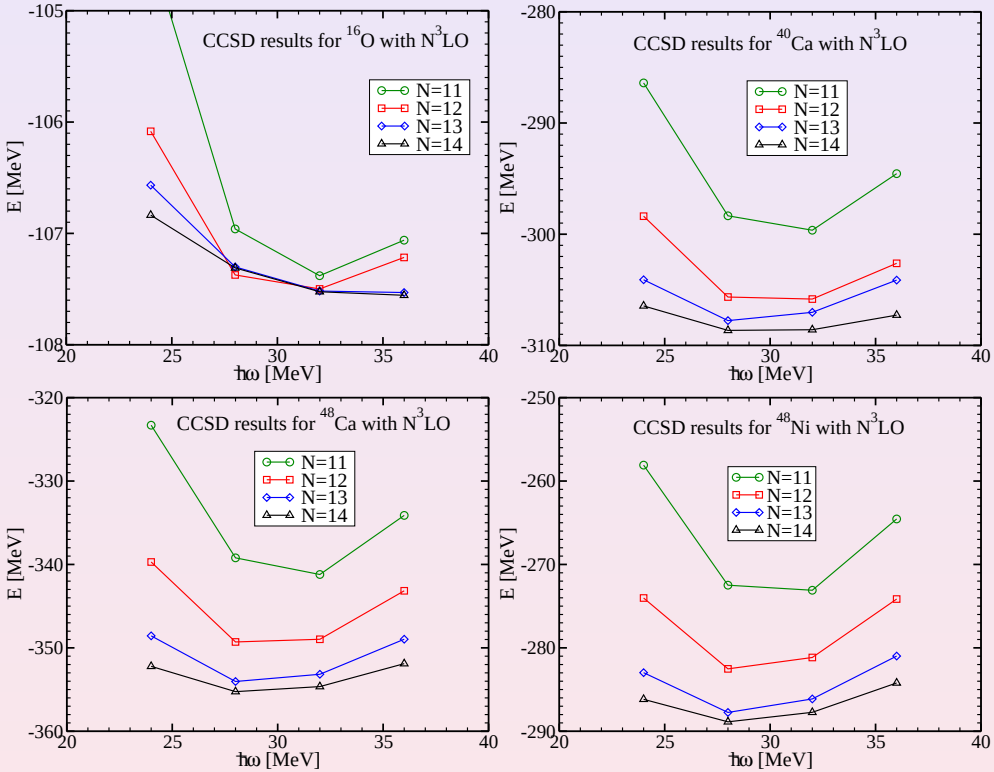

Medium-Mass Nuclei from Chiral Nucleon-Nucleon Interactions, G. Hagen et. al, Phys. Rev. Lett. 101, 092502 (2008)

^{16}O, ^{40}Ca, ^{48}Ca and ^{48}Ni ground state densities

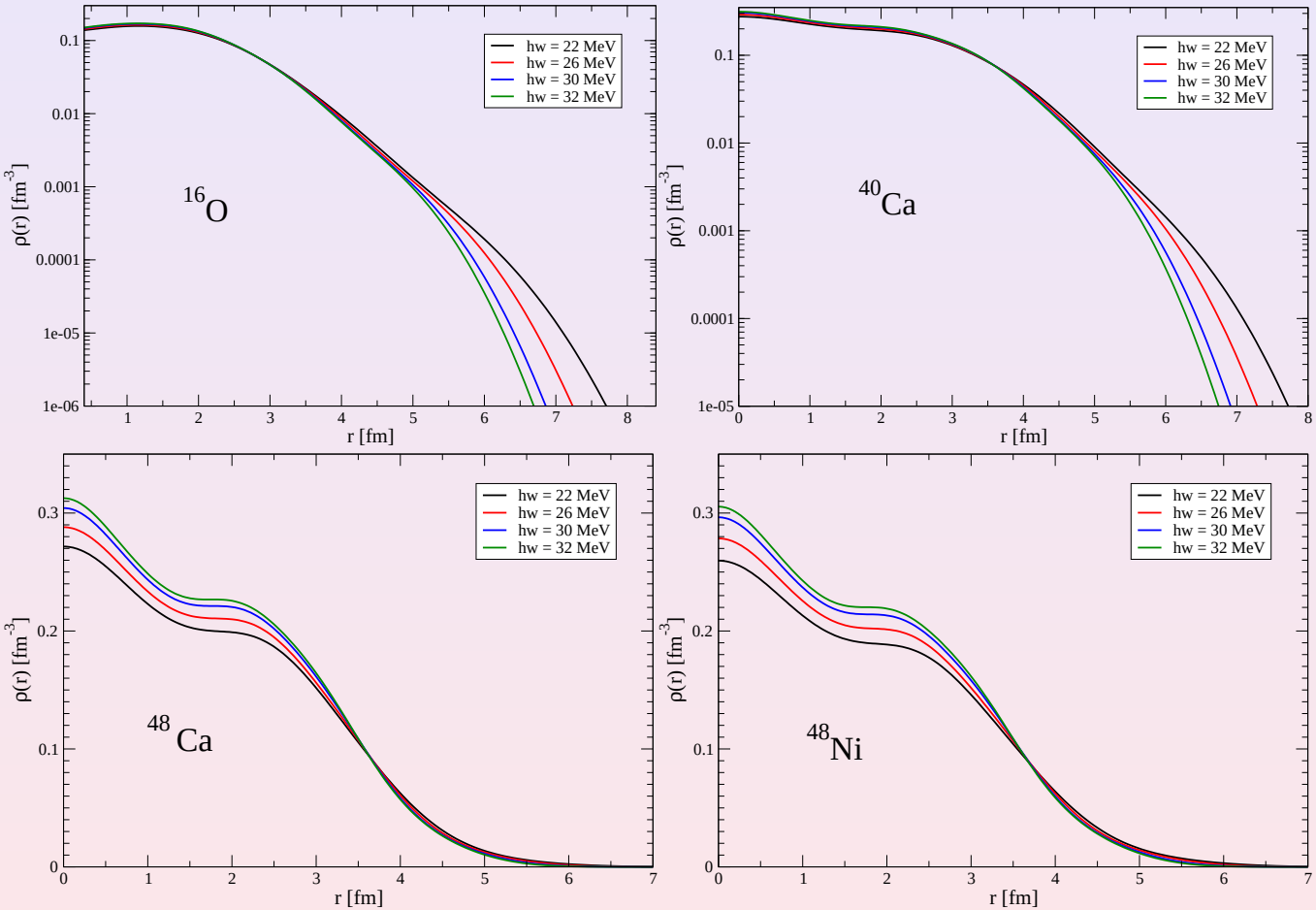

Charge and matter radii/Summary of results

- Charge radii for various nuclei using the chiral N^3LO nucleon-nucleon potential.
- $\sim$ 1MeV/A missing for all nuclei: Size Extensivity!

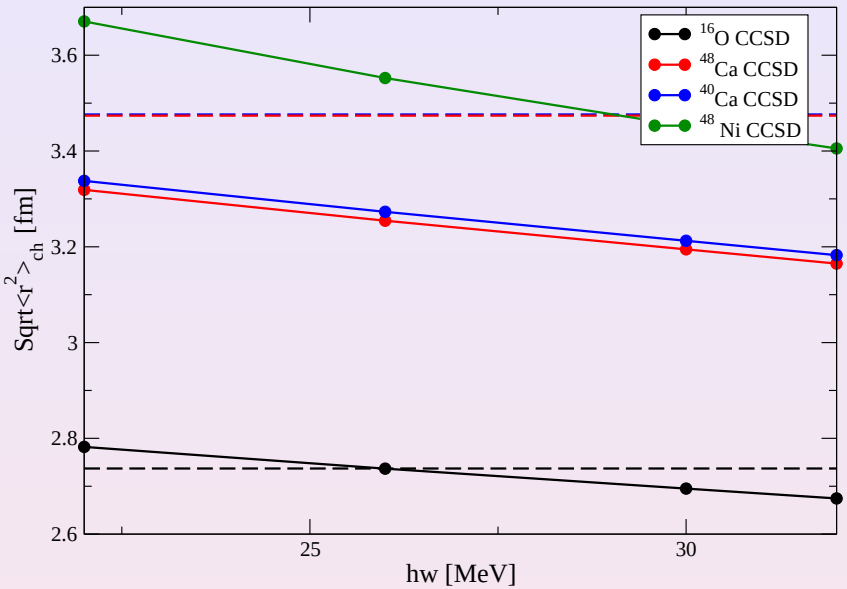

Nucleus	E/A	V/A	Q	$\Delta E/A$	$< r^2 >_{ch}^{1/2}$	$< r^2 >_{ch}^{1/2}$ (Exp)
^{4}He	-5.99	-22.75	0.90	1.08		1.673(1)
^{16}O	-6.72	-30.69	1.08	1.25	2.72(5)	2.737(8)
^{40}Ca	-7.72	-36.40	1.18	0.84	3.25(9)	3.4764
^{48}Ca	-7.40	-37.97	1.21	1.27	3.24(9)	3.4738
^{48}Ni	-6.02	-36.04	1.20	1.21	3.52(15)	?

Triples correction to ground state energies

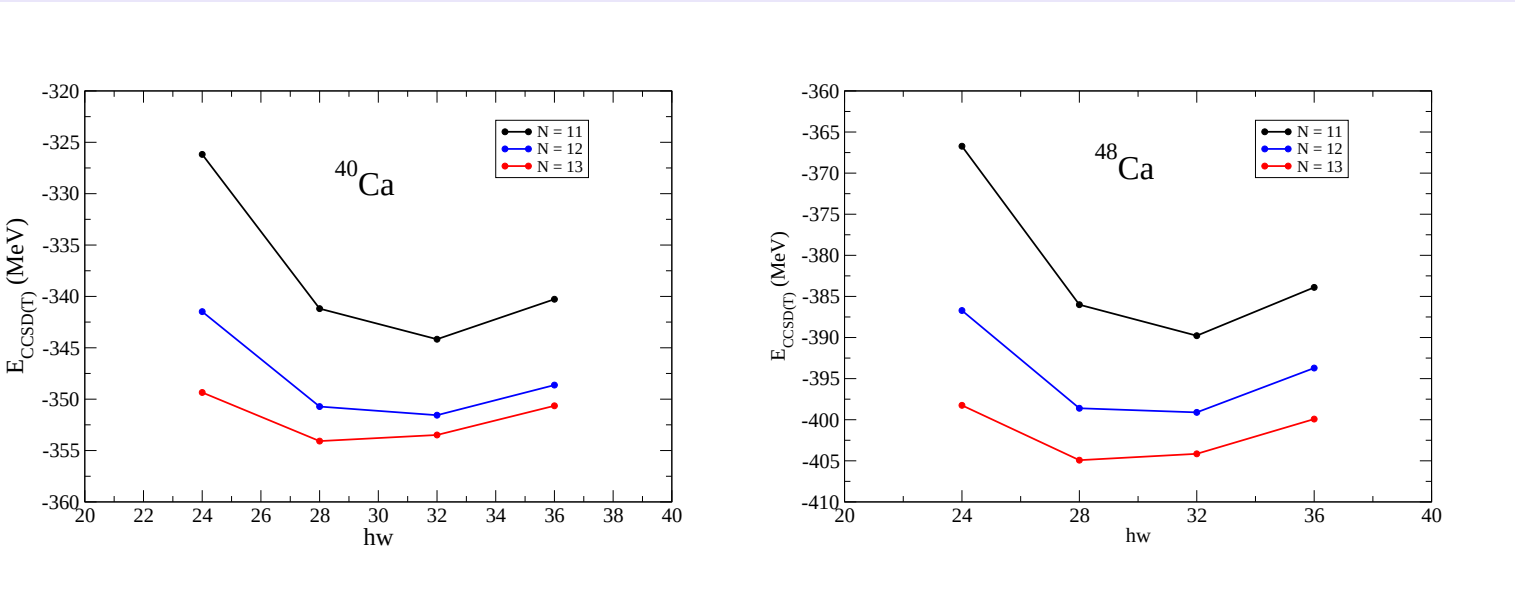

- $\sim$ 500keV/A missing for all nuclei
- Chiral interactions leaves almost no room for three-body forces in medium size nuclei.

	CCSD		ΛCCSD(T)	
Nucleus	E/A	$\Delta E/A$	E/A	$\Delta E/A$
^{16}O	-6.72	1.25	-7.53	0.44
^{40}Ca	-7.72	0.84	-8.62	-0.08
^{48}Ca	-7.40	1.27	-8.22	0.45

^{22}O, ^{24}O, and ^{28}O with chiral interactions

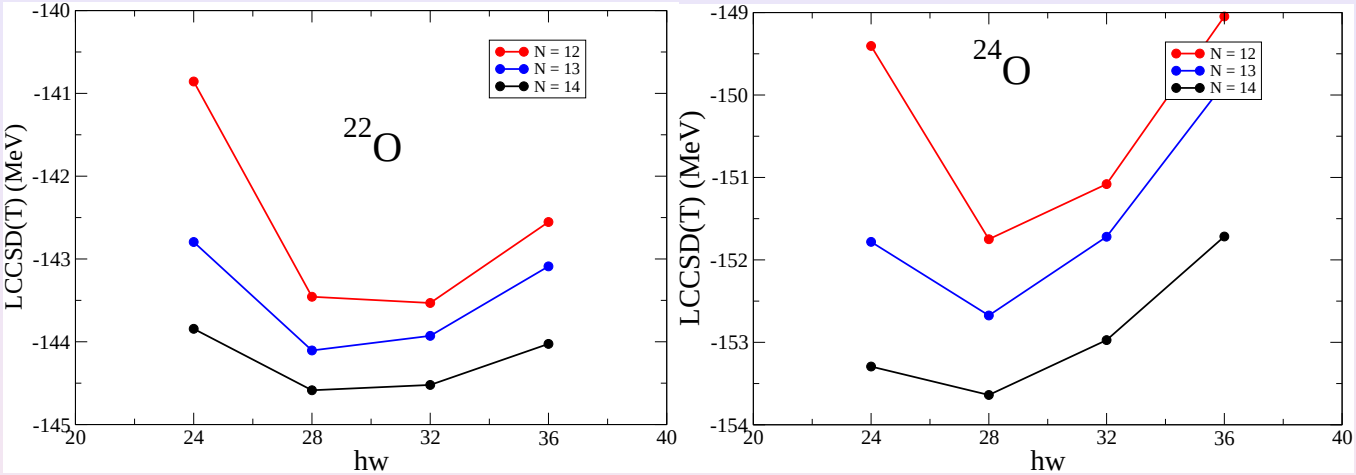

Is ^{28}O stable ?

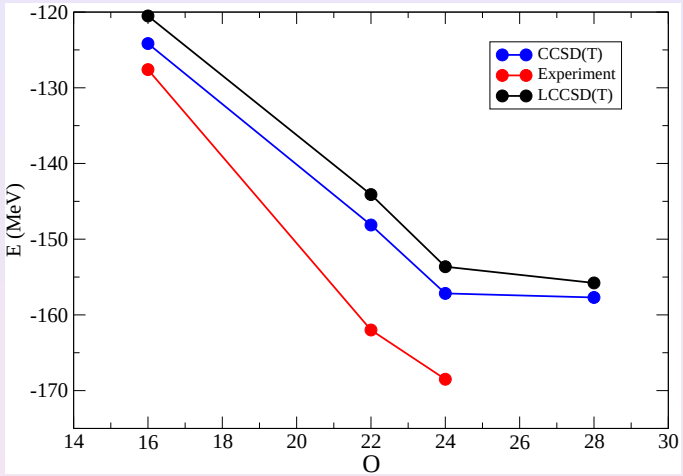

- ΛCCSD(T) results for ^{28}O indicates that it is stable towards $4n$ emission by $\sim$ 2MeV
- Results not converged with respect to model space (N=14)
- What is the binding energy of ^{26}O ? Is this correct?

	CCSD		ΛCCSD(T)	
Nucleus	E/A	$\Delta E/A$	E/A	$\Delta E/A$
^{16}O	-6.72	1.25	-7.53	0.44
^{22}O	-5.72	1.64	-6.59	0.77
^{24}O	-5.58	1.42	-6.42	0.58
^{28}O	-4.86	?	-5.57	?

Ab-initio approach weakly bound and unbound nuclear states

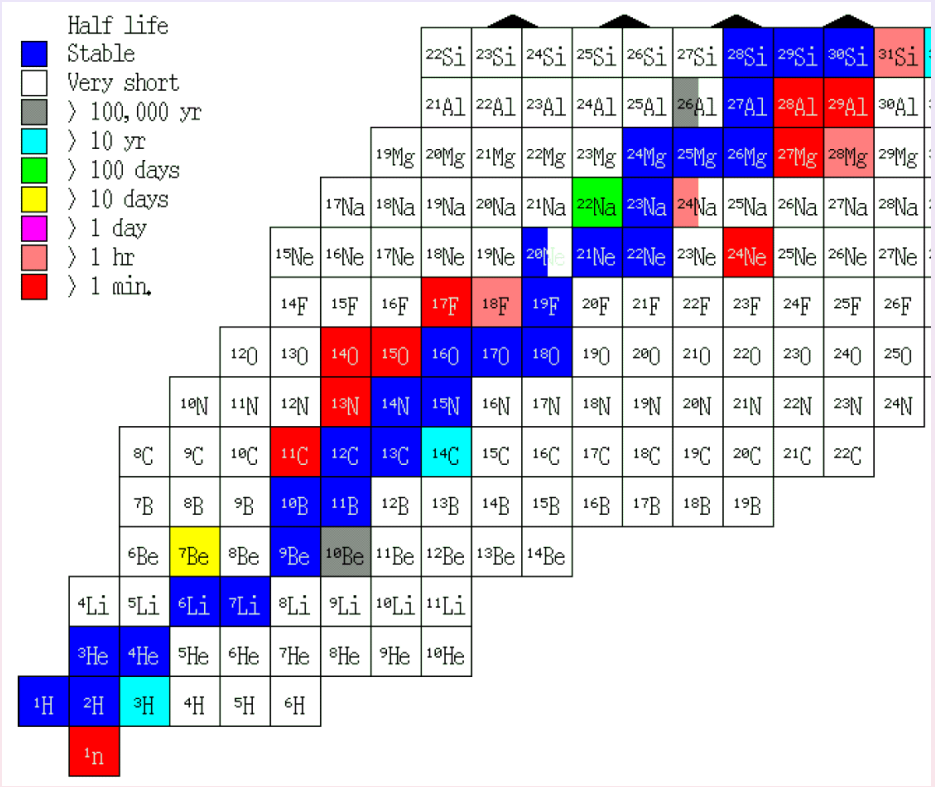

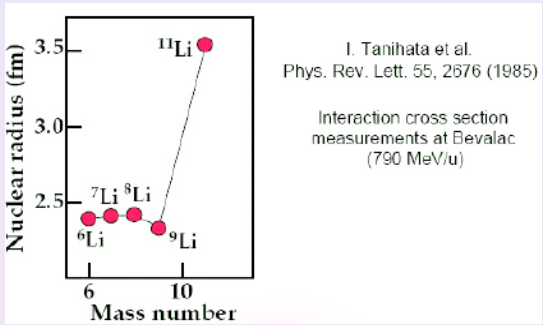

I. Tanihata et al.
Phys. Rev. Lett. 55, 2676 (1985)

Interaction cross section measurements at Bevalac (790 MeV/u)

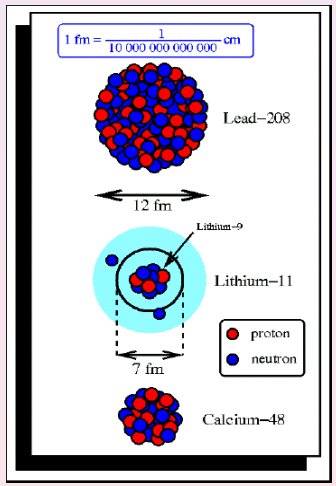

Coupled Cluster for open quantum systems

Open Quantum System.
Coupling with continuum taken into account.

Closed Quantum System.
No coupling with external continuum.

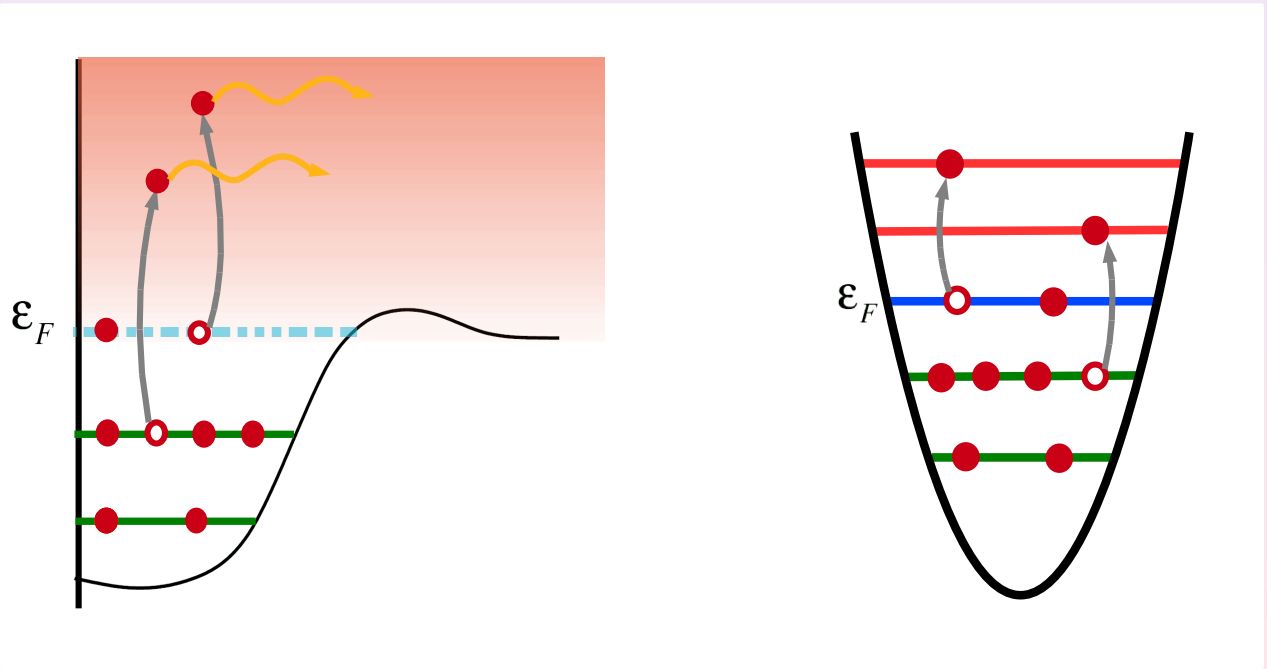

Berggren Single-particle basis

Complex energies requires a generalized completeness relation

$$|\Psi(\mathbf{r},t)|^2 = |\Phi(\mathbf{r})|^2 exp(-\frac{\Gamma}{\hbar}t), \;\; E = E_r - i\Gamma/2.$$

$$\mathbf{1} = \sum_{n=b,d} |\psi_l(k_n)\rangle\langle\tilde{\psi}_l(k_n)| + \int_{L^+} dk\; k^2 |\psi_l(k)\rangle\langle\tilde{\psi}_l(k)|.$$

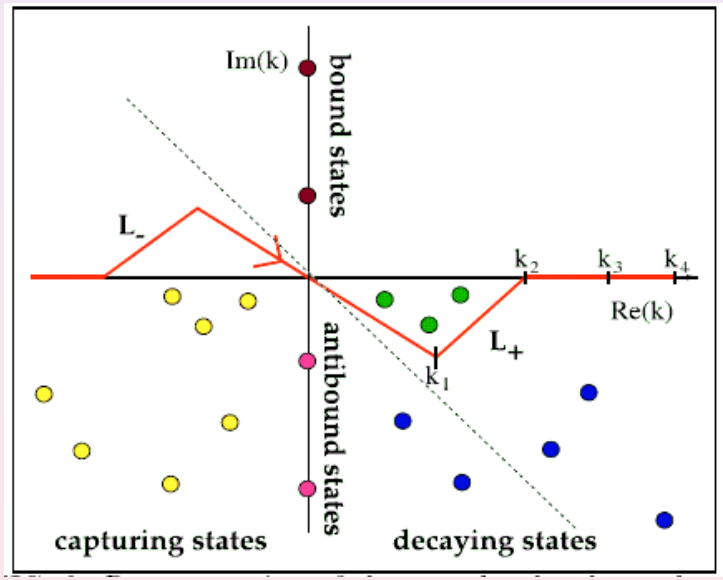

CCSD results for Helium chain using $V_{\mathrm{low}-k}$

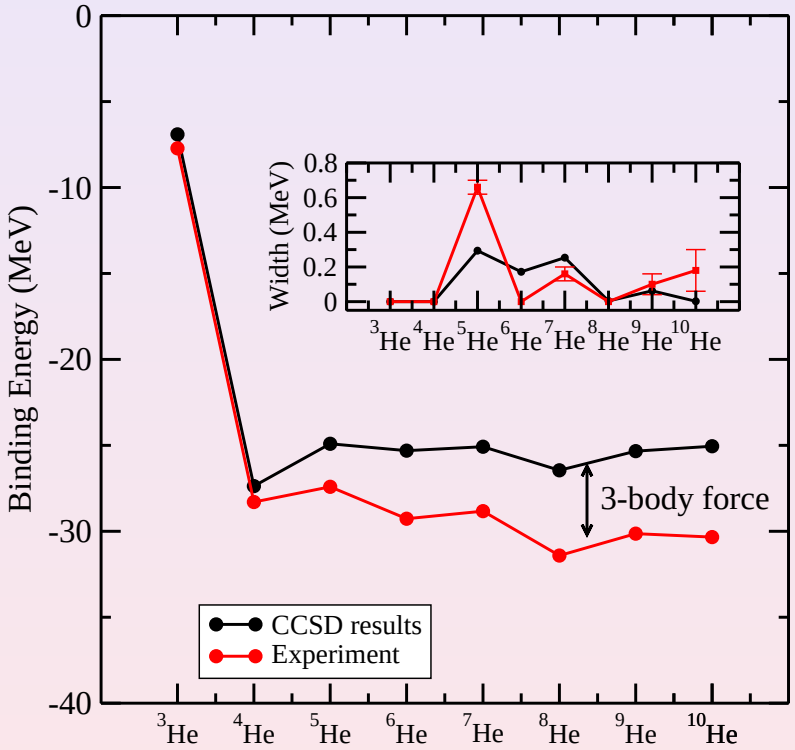

- $V_{\mathrm{low}-k}$ from N3LO with $\Lambda = 1.9\mathrm{fm}^{-1}$.
- G. Hagen et al., Phys. Lett. B 656, 169 (2007). arXiv:nucl-th/0610072.

- First *ab-initio* calculation of decay widths !
- CC unique method for dripline nuclei.
- ~ 1000 active orbitals
- Underbinding hints at missing 3NF?? All results to be revised!

Coupled Cluster and He Isotopes

	^{3}He		^{4}He		^{5}He		^{6}He	
lj	Re[E]	Im[E]	Re[E]	Im[E]	Re[E]	Im[E]	Re[E]	Im[E]
$s-p$	-4.94	0.00	-24.97	0.00	-20.08	-0.54	-19.03	-0.18
$s-d$	-6.42	0.00	-26.58	0.00	-23.56	-0.22	-23.26	-0.09
$s-f$	-6.81	0.00	-27.27	0.00	-24.56	-0.17	-24.69	-0.07
$s-g$	-6.91	0.00	-27.35	0.00	-24.87	-0.16	-25.16	-0.06
Expt.	-7.72	0.00	-28.30	0.00	-27.41	-0.33(2)	-29.27	0.00

CCSD calculation of the $^{3-6}$He ground states with the low-momentum N^{3}LO nucleon-nucleon interaction for increasing number partial waves. The energies E are given in MeV for both real and imaginary parts. Reference state defined so that total spin projection is maximal. Orbits with largest m_j filled first.

Coupled Cluster and He Isotopes

	^{7}He		^{8}He		^{9}He		^{10}He	
lj	Re[E]	Im[E]	Re[E]	Im[E]	Re[E]	Im[E]	Re[E]	Im[E]
$s-p$	-17.02	-0.24	-16.97	-0.00	-15.28	-0.40	-13.82	-0.12
$s-d$	-22.19	-0.12	-22.91	-0.00	-21.34	-0.15	-20.60	-0.02
$s-f$	-24.13	-0.11	-25.28	-0.00	-23.96	-0.06	-23.72	-0.00
$s-g$	-24.83	-0.09	-26.26	-0.00	-25.09	-0.03	-24.77	-0.00
Expt.	-28.83	-0.08(2)	-31.41	0.00	-30.26	-0.05(3)	-30.34	0.09(6)

CCSD calculation of the $^{7-10}$He ground states. 850 single-particle orbitals, $5s5p5d4f44h4i$ proton orbitals and $20s20p5d4f44h4i$ neutron orbitals. For ^{10}He this is approximately 10^{22} basic states.

Exotic Systems

Challenges

Exotic phenomena emerge in weakly bound and resonant many-body quantum systems. These phenomena include ground states that are embedded in the continuum, melting and reorganizing of shell structures, extreme matter clusterizations and halo densities. These unusual features occur in many branches of physics; as examples,in quantum, ultracold atom gases, auto-ionizing or molecules and exotic nuclei. In nuclear physics we find such exotic systems moving away from the valley of nuclear stability towards the drip lines, where the outermost nucleons literally start to drip from the nuclei.

The theoretical description of weakly bound and unbound quantum many-body systems is a challenging undertaking. The proximity of the scattering continuum in these systems implies that they should be treated as open quantum systems where coupling with the scattering continuum can take place. Recent work with Gamow states employed in Hamiltonian diagonalization have shown that these basis states correctly depict properties associated with open quantum systems.

Can we construct effective interactions for such systems?

Complex Scaling, Definitions

In nuclear physics, like in atomic physics, the expansion of many-body wavefunctions on single particle bases, generated by a suitable potential has been common practice. For a given potential the single particle eigenstates form a complete set of states,

$$\mathbf{1} = \sum_b |\psi_{nl}\rangle\langle\psi_{nl}| + \frac{1}{2}\int_{-\infty}^{\infty} dk k^2 |\psi_l(k)\rangle\langle\psi_l(k)|,$$

This completeness relation is known as the *resolution of unity*. The relation also applies to the binary interaction of say two nucleons and their relative motion. The sum is over the bound states in the system, while the integral is over the positive energy continuum states. The infinite space spanned by this basis is given by all square integrable functions on the real energy axis, known as the L^2 space, which forms a Hilbert space. In the case of a confining harmonic oscillator potential there is an infinite number of bound states and no continuum integral.

Complex Scaling, Definitions

The momentum space Schrödinger equation, for relative motion in partial wave l in a central potential, reads

$$\frac{\hbar^2}{2\mu}k^2\psi_{nl}(k) + \frac{2}{\pi}\int_0^\infty dqq^2 V_l(k,q)\psi_{nl}(q) = E_{nl}\psi_{nl}(k).$$

With real momenta the momentum space Schrödinger equation corresponds to a hermitian Hamiltonian. The energy eigenvalues will in this case always be real, corresponding to discrete bound states ($E_{nl} < 0$) and a continuum of scattering states ($E_{nl} > 0$). Resonant and antibound states can never be obtained by directly solving this equation as it stands. In a sense, one can say that the spectrum of a hermitian Hamiltonian does not display all information about the physical system.

Complex Scaling

Generalizing k to the complex k-plane, i.e. $k = \mathrm{Re}[k] + i\mathrm{Im}[k]$, an integral equation for the bound state wavefunctions may be written as

$$\psi_{nl}(k) = \frac{1}{E_{nl} - k^2/2\mu} \frac{2}{\pi} \int_0^\infty dq q^2 V_l(k,q) \psi_{nl}(q).$$

$\psi(k)$ is analytic in the upper half complex k-plane corresponding to the physical energy sheet, except for simple poles at the bound state energies (positive imaginary k) and a cut in the complex E-plane along the real energy axis. The interaction between the particles, $V_l(k,q)$, is assumed to be spherically symmetric without tensor components. Our discussion does not involve the particle spins explicitly.

Complex Scaling

The Fourier-Bessel transform of a non-local potential $V_l(r, r')$ in coordinate space is given by

$$V_l(k, k') = \int_0^\infty dr r^2 \int_0^\infty dr' r'^2 j_l(kr) j_l(k'r') V_l(r, r').$$

In the case of a local potential,

$$V_l(r, r') = \frac{\delta(r - r')}{r^2} V_l(r),$$

yielding

$$V_l(k, k') = \int_0^\infty dr r^2 j_l(kr) j_l(k'r) V_l(r).$$

The interaction in momentum space is given in units of MeVfm^3.

Complex Scaling

Antibound states are not to be interpreted as physical states, i.e. a quantal system cannot be put in such a state. Nevertheless, antibound states close to the scattering threshold may have impact on observables such as phase shifts. For a system with antibound states close to the scattering threshold, a large enhancement of the scattering cross section will take place. This enhancement can be understood in terms of the antibound states.

From a mathematical point of view an antibound state is defined as a pole of the scattering matrix located on the negative imaginary k-axis.

Complex Scaling

Resonant states can be divided into two subclasses; decay and capture states. Decay states are associated with poles of the scattering matrix located in the fourth quadrant of the complex k-plane. They have outgoing boundary conditions at infinity. Capture states are on the other hand associated with poles in the third quadrant of the complex k-plane, and have incoming waves at infinity. Naturally only capture states can be given physical meaning. Capture states may be interpreted as quasi-stationary states formed inside a potential barrier in the positive energy regime.

Complex Scaling

Resonant states will have a definite lifetime before they decay through the barrier. This lifetime varies inversely with the probability of tunneling through the barrier, and the probability of tunneling is given by the width Γ of the resonant states. The width is in turn given by the absolute value of the imaginary part of the resonance energy squared. The closer the resonance energy is to the real energy axis, the smaller the width becomes and the lifetime of the quasi-stationary states increases. This indicates that resonant states with energy close to the real energy axis may have larger impact on observable quantities, e.g. phase shifts and scattering cross sections. Physical decay states are those with positive real energy. Gamow states are to be understood as physical resonant decay states close to the real energy axis, i.e. resonant states with narrow widths.

Complex Scaling

Antibound and resonant states are located on the second (non-physical) energy Riemann sheet. The momentum is a multivalued function of energy; $k(E) = \sqrt{2\mu E}$. Multivalued functions may be represented by Riemann surfaces of branch cuts. The upper half complex k-plane and the lower half complex k-plane maps into the same complex energy plane. This problem is resolved by defining a Riemann surface with two sheets. The physical energy sheet (first sheet) is a mapping of the upper half complex k-plane while the so called *non-physical* energy sheet (second sheet) is a mapping of the lower half complex k-plane.

To reach into the non-physical energy sheet where antibound and resonant states are to be found one has to analytically continue the scattering equations through the cut along the real energy axis and into the lower half complex energy plane. We study here the analytic continuation of the Schrödinger equation into the non-physical sheet by the contour deformation method.

Complex Scaling

In the 1960's Berggren discussed the use of resonant states in eigenfunction expansions of scattering and reaction amplitudes.

The resonant states form an incomplete set of states, for completeness the non-resonant continuum states has to be taken into account. Berggren found that the regularized resonant states along with a set of non-resonant continuum states defined on deformed contours in the complex momentum plane, form a bi-orthogonal set of states. This bi-orthogonal set can in turn be used as expansion basis for various physical quantities, where the resonant character of the system is displayed explicitly.

Complex Scaling

The method Berggren studied is based on analytic continuation of the completeness relation to the complex k-plane by deforming the integration contour.
The sum over bound states are then the residues calculated at the poles of the scattering matrix along the positive imaginary k - axis. The integration along the real axis may then be distorted into some *inversion symmetric* contour, meaning that if k is on C, then $-k$ is also on C. By redefining the completeness relation on distorted contours in the complex k plane, one can show by using Cauchy's residue theorem that the summation over discrete states will in general include bound, antibound and resonant states. By this procedure the norm integral of the resonant states is regularized along the distorted contours.
The eigenfunctions defined along distorted contours form a *biorthogonal* set, and the normalization follows the generalized c-product

$$\langle\langle\psi_{nl}|\psi_{n'l}\rangle\rangle \equiv \langle\psi^*_{nl}|\psi_{n'l}\rangle = \delta_{n,n'}\,.$$

General Completeness Relation

The most general completeness relation on an arbitrary *inversion symmetric* contour $C = C^+ + C^-$ can then be written as

$$\mathbf{1} = \sum_{n \in \mathbf{C}} |\psi_{nl}\rangle\langle\psi^*_{nl}| + \int_{C^+} dz |\psi_l(z)\rangle\langle\psi^*_l(z)|,$$

where C^+ is the distortion of the positive real k-axis, and C^- is the distortion of the negative real k-axis.

$$\int_{C^-} dz |\psi_l(z)\rangle\langle\psi^*_l(z)| = \int_{C^+} dz |\psi_l(z)\rangle\langle\psi^*_l(z)|.$$

The summation is over all discrete states (bound, virtual and resonant states) located in the domain $\mathbf{C}$, defined as the area above the contour C, and the integral is over the non-resonant complex continuum defined on C^+.

Complex Scaling

Here the symmetry of the integrand has been taken into account, that is

$$\int_{C^-} dk k^2 |\psi_l(k)\rangle\langle\psi_l^*(k)| = \int_{C^+} dk k^2 |\psi_l(k)\rangle\langle\psi_l^*(k)|.$$

The summation is over all discrete states (bound, antibound and resonant states) located in the domain **C**, defined as the area above the contour C, and the integral is over the non-resonant complex continuum defined on C^+. The space spanned by the basis includes all square integrable functions defined in the domain **C**, defining a generalized Hilbert space.
In analytic continuation of integral equations we state the general rule
Continuing an integral in the complex plane, the moving singularities of the integrand must not intercept the integration contour.

A modified contour

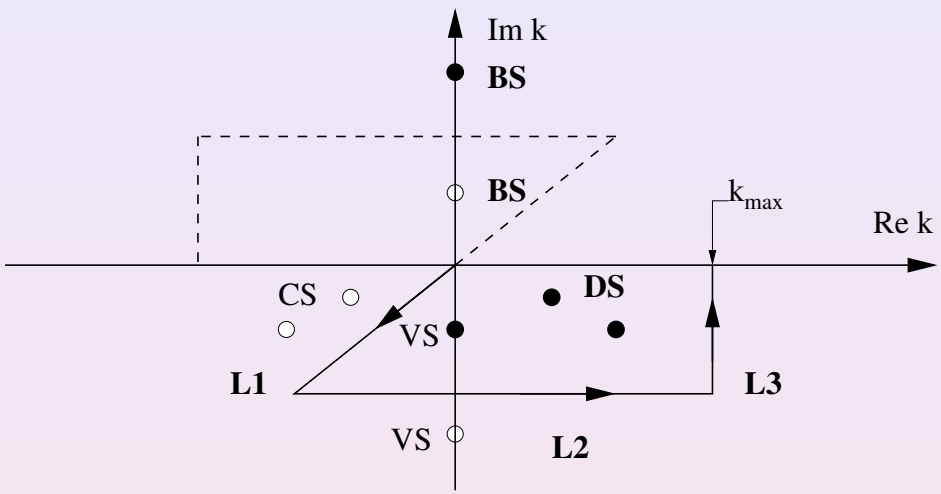

The contour C_2^+

- The line segment L_1 is given by a rotation $z_1 = k_1 \exp(-i\theta)$
- $k_1 \in [0, b]$, L_2 is given by a translation $z_2 = k_2 - ib\sin(\theta)$ where $k_2 \in [b\cos(\theta), k_{\max}]$ and
- b determines the translation into the lower-half k-plane and L_3 by $z_3 = k_{\max} - ic$ where $c \in [b\sin(\theta)0]$.

Sketch of two possible contours

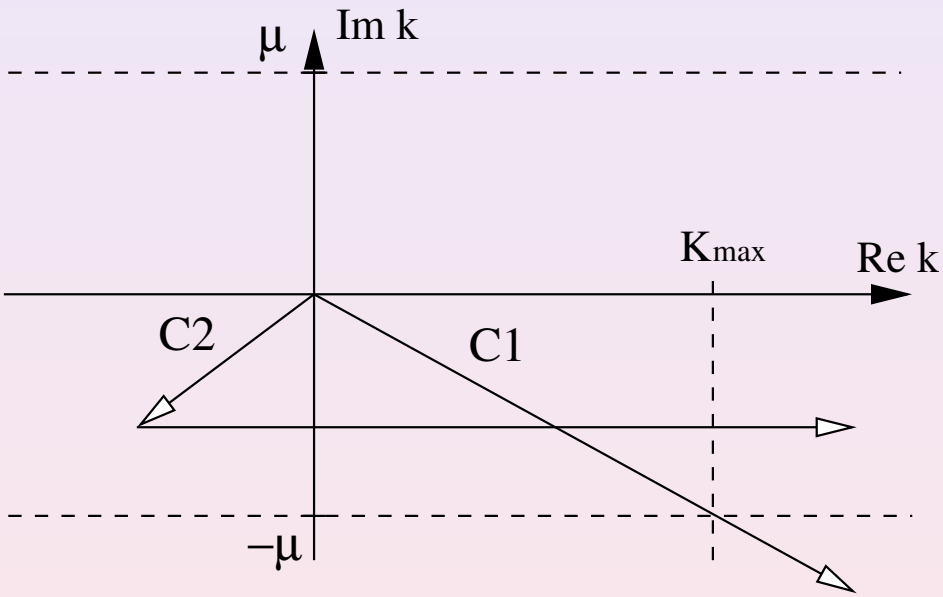

Interaction Singularity

For $k, k' > \mu_A / \tan(\theta) = k_{\max}$ the contour C_1^+ will pass through the singularity of the interaction and Cauchy's integral theorem cannot be applied.

Complex interaction, the t-matrix

We can then obtain a complex t-matrix defined in operator form by

$$t(\omega) = V + VG(\omega)V,$$

with

$$G(\omega) = \sum_b \frac{|\psi_b\rangle\langle\psi_b|}{\omega - E_b} + \int_0^\infty dE_c \frac{|\psi_c\rangle\langle\psi_c|}{\omega - E_c},$$

or in full glory (real k, k')

$$t_l(k,k',\omega) = V_l(k,k') + \frac{4}{\pi^2}\sum_\alpha \int_C \int_{C'} dz\, dz'\, z^2 z'^2 V_l(k,z)\frac{\psi_\alpha(z)\psi_\alpha(z')}{\omega - E_\alpha} V_l(z',k'),$$

Here C is either C_1^+ or C_2^+. This applies to C' as well. The last equation can be solved via matrix inversion or as an eigenvalue problem.

t-Matrix for Malfliet-Tjon like potential

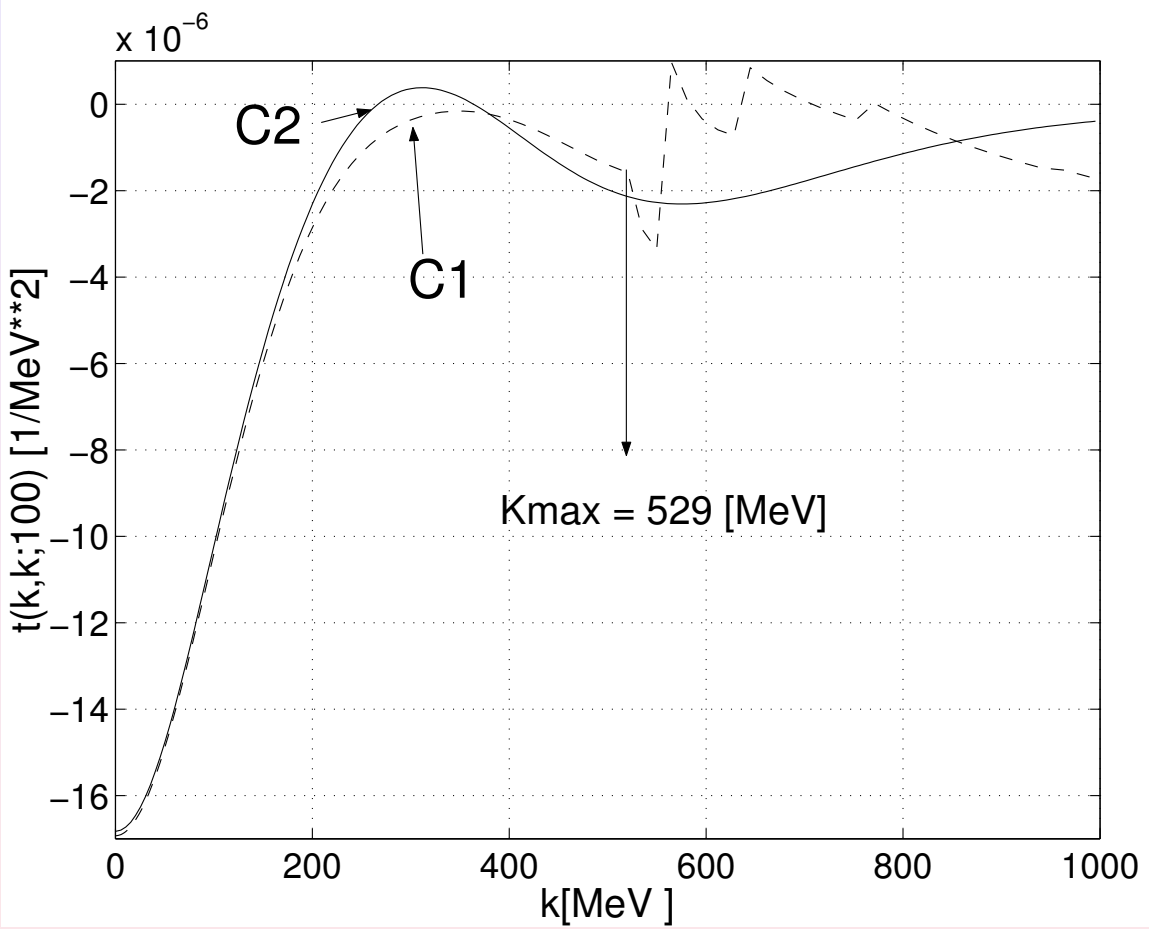

Two-body Matrix Elements I

The renormalized nucleon-nucleon interaction in an arbitrary two-particle basis in the laboratory frame is given by

$$\langle ab|V_{\mathrm{low-k}}|cd\rangle = \langle (n_a l_a j_a t_{z_a})(n_b l_b j_b t_{z_b}) JT_z| \, V_{\mathrm{low-k}} \, |(n_c l_c j_c t_{z_c})(n_d l_d j_d t_{z_d}) JT_z\rangle \, . \tag{19}$$

The two-body state $|ab\rangle$ is implicitly coupled to good angular momentum J. The labels $n_{a\ldots d}$ number all bound, resonant and discretized scattering states with orbital and angular momenta $(l_{a\ldots d}, j_{a\ldots d})$.
In order to efficiently calculate the matrix elements of Eq. (19), we introduce a two-particle harmonic oscillator basis completeness relation

$$\sum_{\alpha \leq \beta} |\alpha\beta\rangle\langle\alpha\beta| = \mathbf{1}, \tag{20}$$

where the sum is not restricted in the neutron-proton case. We introduce the greek single particle labels α, β for the single-particle harmonic oscillator states in order to distinguish them from the latin single-particle labels a, b referring to Gamow states.

Two-body Matrix Elements II

The interaction can then be expressed in the complete basis of Eq. (20)

$$V_{\rm osc} = \sum_{\alpha\leq\beta}\sum_{\gamma\leq\delta} |\alpha\beta\rangle\langle\alpha\beta|V_{\rm low-k}|\gamma\delta\rangle\langle\gamma\delta|, \tag{21}$$

where the sums over two-particle harmonic oscillator states are infinite. The expansion coefficients

$$\langle\alpha\beta|V_{\rm low-k}|\gamma\delta\rangle = \left\langle (n_\alpha l_\alpha j_\alpha t_{z_\alpha})(n_\beta l_\beta j_\beta t_{z_\beta})JT_z \right| V_{\rm low-k} \left|(n_\gamma l_\gamma j_\gamma t_{z_\gamma})(n_\delta l_\delta j_\delta t_{z_\delta})JT_z\right\rangle ,$$

represent the nucleon-nucleon interaction in an antisymmetrized two-particle harmonic oscillator basis, and may easily be calculated using the well known Moshinsky transformation coefficients.

Two-body Matrix Elements III

Matrix elements of Eq. (19) are calculated numerically in an arbitrary two-particle Gamow basis by truncating the completeness expansion of Eq. (21) up to N harmonic oscillator two-body states

$$\langle ab|V_{\rm osc}|cd\rangle \approx \sum_{\alpha\leq\beta}^{N}\sum_{\gamma\leq\delta}^{N}\langle ab|\alpha\beta\rangle\langle\alpha\beta|V_{\rm low-k}|\gamma\delta\rangle\langle\gamma\delta|cd\rangle. \tag{22}$$

The two-particle overlap integrals $\langle ab|\alpha\beta\rangle$ read

$$\langle ab|\alpha\beta\rangle = \frac{\langle a|\alpha\rangle\langle b|\beta\rangle - (-1)^{J-j_\alpha-j_\beta}\langle a|\beta\rangle\langle b|\alpha\rangle}{\sqrt{(1+\delta_{ab})(1+\delta_{\alpha\beta})}} \tag{23}$$

for identical particles (proton-proton or neutron-neutron states) and

$$\langle ab|\alpha\beta\rangle = \langle a|\alpha\rangle\langle b|\beta\rangle \tag{24}$$

for the proton-neutron case.

Two-body Matrix Elements IV

The one-body overlaps $\langle a|\alpha\rangle$ are given by,

$$\langle a|\alpha\rangle = \int d\tau\, \tau^2 \varphi_a(\tau) R_\alpha(\tau)\, \delta_{l_a l_\alpha} \delta_{j_a j_\alpha} \delta_{t_a t_\alpha}\,, \tag{25}$$

where φ_a is a Gamow single-particle state and R_α is a harmonic oscillator wave function. The radial integral is either evaluated in momentum or position space, indicated by the integration variable τ. The important point to notice is that the only numerical calculations involving Gamow states are the overlaps of Eq. (25). Hence, this expansion provides a simple analytical continuation of the nuclear interaction in the complex k-plane. More precisely, the expansion coefficients of Eq. (22) can always be calculated with real harmonic oscillator wave functions, and in the case of Gamow functions spanning a complex contour L^+ (as in the momentum space representation), it is only the overlap integrals of Eq. (25) which are analytically continued in the complex plane. These one-body overlap integrals converge in all regions of the complex plane which are of physical importance, due to the gaussian fall off of the harmonic oscillator wave functions.

$\hbar\omega$ dependence of the real part of the ^{5}He ground state energy

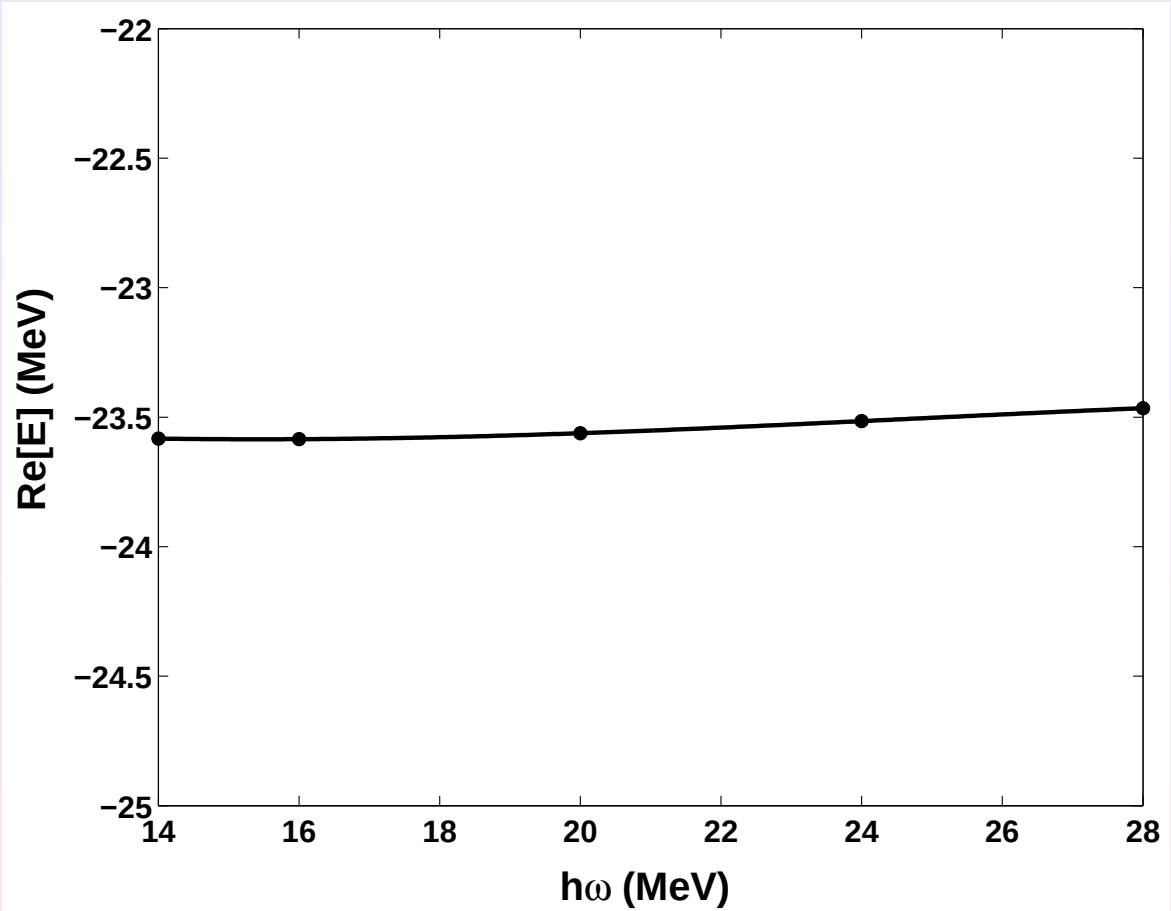

$\hbar\omega$ dependence of the imaginary part of the ^{5}He ground state energy

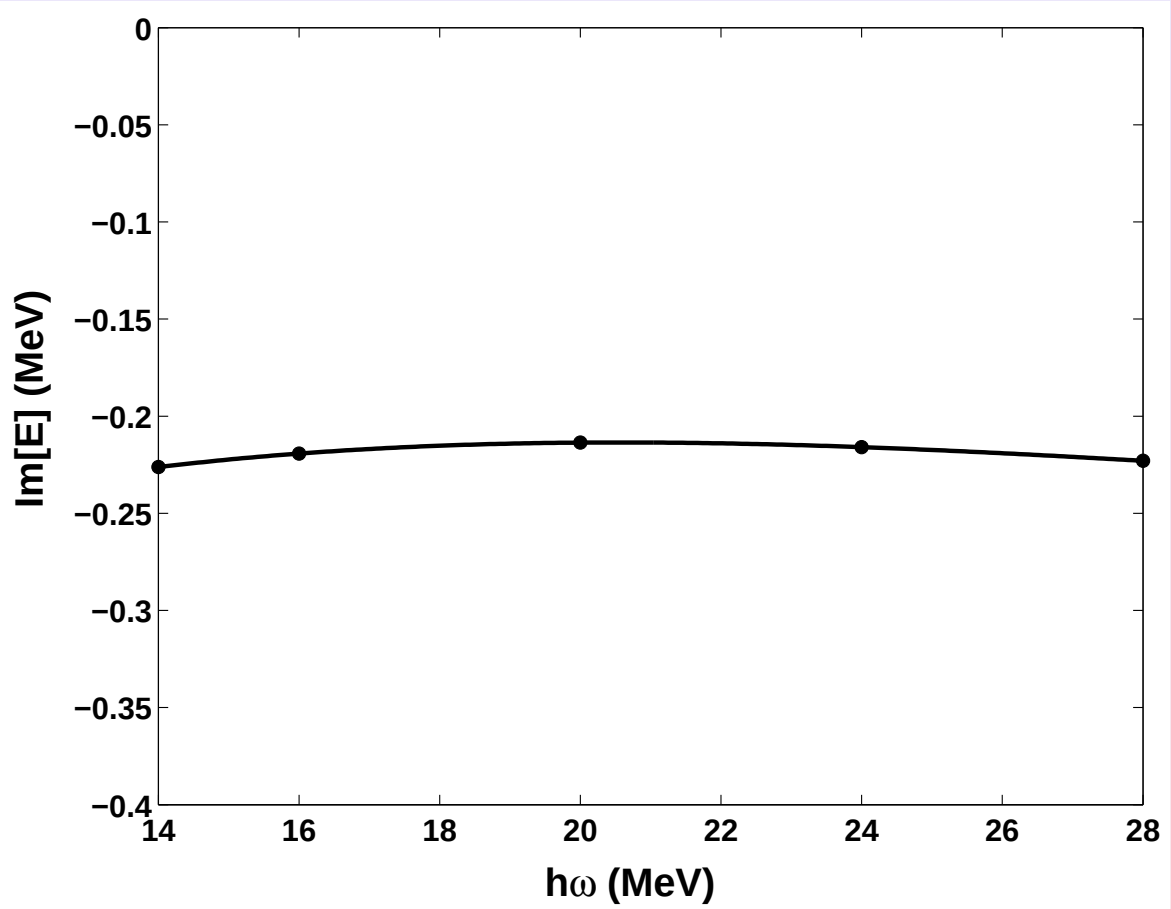

Convergence of the real part of the ^{5}He ground state energy

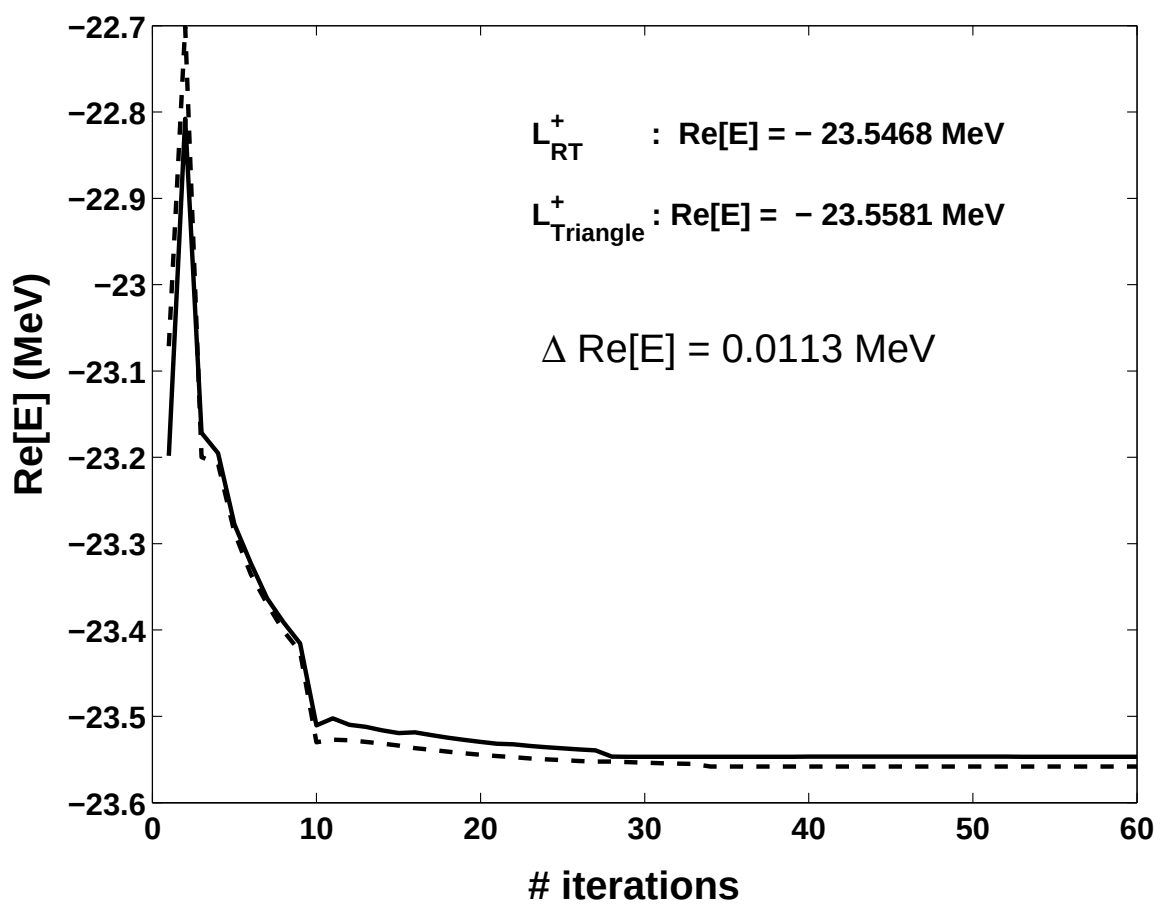

Convergence of the imag part of the ^{5}He ground state energy

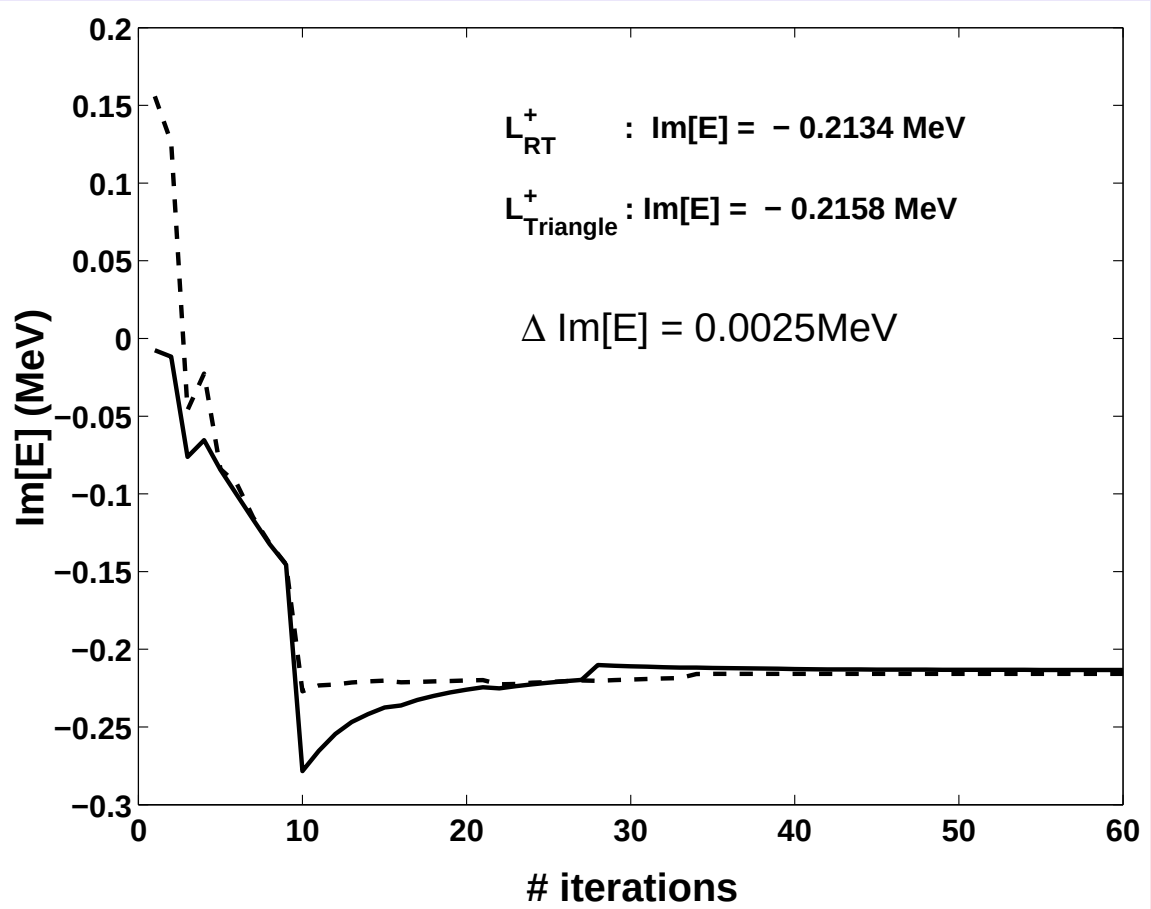

Conclusion

- Coupled Cluster meets few-body benchmark calculations.
- J-coupled CCSD and CCSD(T) code has been derived and implemented. Coupled cluster approach to medium mass and driplines with bare interactions!
- Derived and implemented Equation of Motion CCM; calculation of density distributions and radii.
- CCM has been succesfully applied to the description of weakly bound and unbound helium isotopes.
- We have a tool to attack the structure and properties of dripline and medium mass nuclei !

Future perspectives

- Location of dripline in the Oxygen chain ?
- Revisit Helium chain with 3NF. Spin-orbit splitting in He7 and He9.
- Matter and charge radii of ^{11}Li.
- Excited states and matter densities for dripline nuclei.
- Coupled Cluster approach to nuclear matter.
- Construction of effective interaction for shell-model calculations.
- Coupled-Cluster approach to nuclear reactions; CC-LIT and construction of optical potentials from folding procedures.
- We are developing a J-coupled CCSDT code.
- Ab-initio description of ^{56}Ni, ^{100}Sn and ^{208}Pb within reach!